Open Access

InfoMat

www.info-mat.org
Vol.2·NO.5·2020

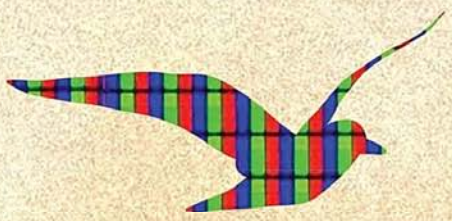

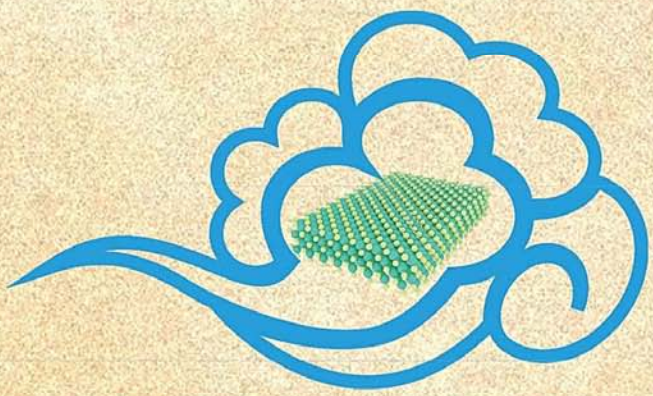

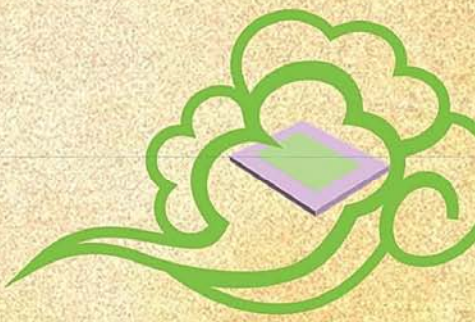

University of Electronic Science & Technology of China
UESTC
1956

WILEY

Received: 28 December 2019 | Revised: 8 February 2020 | Accepted: 16 February 2020

DOI: 10.1002/inf2.12106

REVIEW ARTICLE

WILEY

Optical properties and applications of two-dimensional CdSe nanoplatelets

Jiahao Yu[1,2] | **Rui Chen**[1]

[1]Department of Electrical and Electronic Engineering, Southern University of Science and Technology, Shenzhen, Guangdong, China

[2]Harbin Institute of Technology, Harbin, China

Correspondence
Rui Chen, Department of Electrical and Electronic Engineering, Southern University of Science and Technology, Shenzhen, Guangdong 518055, China.
Email: chenr@sustech.edu.cn

Funding information
National Natural Science Foundation of China, Grant/Award Number: 11574130; Shenzhen Science and Technology Innovation Commission, Grant/Award Numbers: JCYJ20180305180553701, KQJSCX20170726145748464, KQTD2015071710313656

Abstract

Compared with zero-dimensional quantum dots and one-dimensional nanorods, two-dimensional nanoplatelets exhibit many unique optical properties. Due to strong quantum confinement in only one direction and the large lateral size, the CdSe nanoplatelets show large exciton binding energy, giant oscillator strength, narrow emission, large absorption cross-section, and large optical gain. In this review, the development of synthesis technology of nanoplatelets is first briefly introduced. Subsequently, the optical properties of CdSe nanoplatelets and their heterostructures are reviewed, including absorption and photoluminescence, carrier dynamics, optical gain, and nonlinear properties. These optical properties are affected by size, material and structure. At last, the main applications of CdSe nanoplatelets in recent years are introduced, including light-emitting diodes, lasers, light harvesting, photocatalysis, and sensing.

KEYWORDS

CdSe nanoplatelets, optical property, semiconductor nanocrystal, two-dimensional material

1 | INTRODUCTION

In 1981, the quantum size effect was first demonstrated in semiconductor nanocrystals, which opened the door to the huge research system for semiconducting nanomaterials.[1] The size-dependent quantized electronic energy levels make it possible to control the energy gap and other properties of semiconductors. Initially, the optical and electronic properties of semiconductor nanocrystals were studied through the samples that were grown inside glass.[2,3] However, such semiconductor nanocrystals embedded in glass suffer serious strain, thus hindering the progress of many studies. The nearly monodisperse CdE (E = S, Se, Te) semiconductor nanocrystallites were synthesized in 1993, which make the research of semiconductor nanomaterials step into a new stage.[4] With the rapid development of solution synthesis technology, large number of spherical semiconductor nanocrystals have emerged first, which is also called quantum dots (QDs). Through the selection of precursor materials and the control of synthesis conditions, QDs of various material systems have been successfully synthesized. The changes in the radius and composition of QDs enable its light emission wavelength adjustable, which can cover from ultraviolet to near-infrared region.[5] The coating of QDs by organic ligands has passivated the surface dangling bonds, which results in improved quantum yield (QY). The emergence of core-shell heterojunction structure has further enable the property control of QDs. The combination of different core and shell materials can change the spatial distribution and the wave function of carriers.[6,7] This structural control can ultimately be

reflected in changes to the photophysical properties of QDs, such as reducing Auger recombination of multiexcitons and increasing the Stokes shift.[8-10] After nearly 30 years of development, QDs have derived a variety of applications. The adjustable emission color and high photoluminescence (PL) QY make QDs a popular research material in the field of display and light-emitting diodes (LED).[11-13] Some biocompatible QDs are used for fluorescent labeling, biosensing.[14,15] In addition, QDs with high quality and QY can be used for laser application.[16-18]

It is known that these unique photophysical properties of QDs are ascribed by the quantum confinement effects. The electrons in QDs are confined in three dimensions (3D), which is the main reason for the difference of properties between QDs and bulk materials. Therefore, in addition to composition, structure, and size, changing the dimension of quantum confinement is another effective method to manipulate the properties of semiconductor nanocrystals. As a common II-VI semiconductor, cadmium selenide (CdSe) is the most widely studied material currently. Various new synthetic methods and structures have been fabricated based on CdSe. In 2000, Peng successfully controlled the shape of semiconductor nanocrystals during synthesis and demonstrated the elongated nanorods.[19] Compared to QDs, nanorod shows quantum confinement effects only in two dimensions (2D). The special shape of nanorod induces many interesting optical properties, such as larger absorption cross-section, and polarization effects.[20]

In 2006, a new shape of colloidal semiconductor nanocrystals appeared.[21] The 2D CdSe nanoplatelets (NPLs) has a large lateral size, while it has only a few molecular layers in thickness. After the 3D-confined QDs and 2D-confined nanorod have been realized, the one-dimensional (1D)-confined NPLs fill the other blank of colloidal semiconductor nanocrystal system. Compared with QDs, NPLs not only have the properties normally found in semiconductor nanocrystal, they also exhibit many other interesting and attractive optical properties, including narrow emission, large exciton binding energy, giant oscillator strength, large absorption cross-section, fast fluorescence lifetime, and large optical gains.[22-24] In colloidal QDs system, heterostructures are used to optimize or tune the optical properties. Similar method is also used for CdSe NPLs. Core-shell NPLs appeared in the early days.[25,26] After that, an interesting core-crown structure appeared.[27,28] This provides a novel method for tuning the optical properties of colloidal semiconductor nanocrystals, which cannot be achieved in QDs. In addition, complex heterostructures such as core/crown/shell NPLs, and core/multi-crown NPLs have also been synthesized.[29,30] Due to the ultra-thin planar structure of NPLs, there exist self-stacking phenomena, which will also have some impact on their optical properties.[31,32]

The CdSe NPLs have extremely narrow emission, which means that the emission color is very pure, thus they have been considered as a good light-emitting material in displays and LEDs.[33,34] High optical gain is another excellent optical property of CdSe NPLs, which enables NPLs for amplified spontaneous emission (ASE) with low threshold.[35] When combined with a high quality optical cavity, low threshold lasers can be realized. In recent years, many NPLs and their complex heterostructures have been applied to lasers, and continuous-pumped lasers have been reported at room temperature.[30,36,37] In addition, the large surface area of NPLs is also a good platform for the sensing and photocatalysis application.[38,39]

In the first part of this review, the development of synthetic technology of colloidal CdSe NPLs and heterostructures will be briefly introduced. Then we will focus on the unique optical properties of the NPLs, and summarize how the structure influences the optical properties. Next, applications based on CdSe NPLs will be mentioned. In the last, there will be a conclusion and outlook of the colloidal CdSe NPLs.

2 | SYNTHESIS OF NANOPLATELETS

The first colloidal CdSe nanoribbons were successfully synthesized in 2006 by Joo et al.[21] The nanoribbons with wurtzite structure are synthesized from the reaction of $CdCl_2$ and octylammonium selenocarbamate in octylamine at low temperature. The nanoribbons have a uniform thickness of 1.4 nm and show a narrow full width at half-maximum (FWHM) (approximately 70 meV). In 2008, the CdSe NPLs with zinc blende structure was synthesized by Ithurria et al.[40] First, cadmium myristate and selenium mesh precursors in the presence of a noncoordinating solvent to form the platelets nucleation at a certain temperature. The temperature at this stage is the key to control the thickness of the NPLs. At the precise controlled temperature, the injection of the cadmium acetate leads to a lateral growth. The related anisotropic growth mechanism that breaks symmetry has been studied extensively.[41,42] NPLs with 3 to 5 monolayers (MLs) thicknesses can be obtained through this method. Moreover, the aspect ratio, lateral size can be controlled by different reaction time and amount of precursors. NPLs with a thin thickness (2, 3 MLs) usually have a lower QY and are accompanied by a larger proportion of deep level emissions, so they are not commonly used for practical research.[43] In recent years, thicker NPLs have

been synthesized using the improved methods. In 2018, Chu et al used the colloidal atomic layer deposition (c-ALD) method to grow the CdSe layers on the surface of the 4 MLs CdSe NPLs, thereby obtaining thicker CdSe NPLs up to 11 MLs.[44] Christodoulou et al used the 4 MLs CdSe NPLs as initial materials and increased the thickness to 8 MLs by adding $CdCl_2$ in a two-step reaction scheme at high temperature.[45]

For QDs, the heterostructure formed by epitaxial growth of another semiconductor material can enhance or tune the optical properties.[6] For example, QDs with a core-shell structure can achieve higher QY, and the design of the shell structure can influence the spatial distribution of carriers, thereby achieving special applications. For NPLs, this core-shell structure can also be implemented. In 2012, Ithurria and Talapin successfully deposited CdS shell on CdSe NPLs by the c-ALD method, and formed CdSe/CdS core-shell structure.[25] This method achieves shell growth by alternately depositing cation and anion monoatomic layers. The process relies on sequential phase transfer of NPLs between immiscible polar and nonpolar phases. The shell synthesized in this way has a very precise number of monolayers. Although this layer-by-layer growth method can accurately design the structural parameters of the shell layer. Unfortunately, once a thick shell layer is needed, this method becomes complicated and time-consuming. Moreover, multiple purification steps after each layer of shell deposition lead to a dramatic decrease in PLQY and poor photostability. In 2012, Mahler et al proposed a "one-pot" method for continuous growth of the shell.[46] The reaction of thioacetamide and octylamine serves as the source of sulfur, and hydrogen sulfide is generated to react with the cadmium acetate added later to form a shell. The above methods are performed at room temperature. In recent years, there have been reports of synthesizing CdS or ZnS shells at high temperatures.[26,47] These shells synthesized at high temperatures have been confirmed to have better crystal quality and therefore exhibit better optical properties, such as higher QY and stability.

There is a special type in the heterostructure of NPLs, which is called the core/crown NPLs heterostructure. In this structure, CdS or other semiconductor materials only grow laterally around the CdSe NPLs core. Therefore, the formation of a heterostructure does not change the overall thickness, which means that the quantum confinement effect in the vertical direction of the NPLs will not be affected. The core/crown CdSe/CdS NPLs was reported to be synthesized in 2013.[27,28] In this method, elemental sulfur dissolved in octadecene is used as sulfur precursor, and the cadmium precursor is the mixture of cadmium acetate and oleic. The presence of acetate is considered necessary for causing lateral extension. By changing the material composition of core and crown, many different NPLs heterostructure were synthesized. For example, the type-II CdSe/CdTe core/crown NPLs and inverted type-I CdS/CdSe core/crown NPLs have been reported.[48,49] In addition to pure material selection, there are some complex heterostructures. By synthesizing the alloy shell or multi-shell, the core optical properties of the NPLs can be further optimized. In 2018, a CdSe/CdS@$Cd_{1-x}Zn_xS$ colloidal core/crown @ alloyed-shell NPLs was reported.[29] This structure formed by layer-by-layer grown and composition-tuned gradient $Cd_{1-x}Zn_xS$ shells on CdSe/CdS core/crown seeds.

Doping is a method to tune the optical and electrical properties of semiconductor nanocrystals, which have been reported in QDs. Metal ions are commonly used for doping, including Mn, Cu, Ag, and so forth. They have also been successfully doped into NPLs structure in recent years. In 2017, Sharma et al used the hot injection-based nucleation doping method to obtain the copper-doped CdSe NPLs.[50] After the formation of seeds of the NPLs, the precursor of the dopant was added, and then the cadmium acetate was quickly added to start the lateral growth of the NPLs. This method is also used to synthesize Hg-doped CdSe NPLs.[51] In addition to the high temperature hot injection method, one can also realize doping through cation exchange. Recently, a precise control of the doping level was reported through the cation exchange method. The tunable PL emission in the visible-to-NIR spectral region was achieved by the Cu doped-CdSe NPLs with different doping levels.[52]

3 | OPTICAL PROPERTIES OF CDSE NANOPLATELETS

3.1 | Absorption and photoluminescence

Figure 1A shows the absorption and PL spectra of CdSe NPLs with different thickness. It can be seen that all these absorption spectra have two distinct absorption peaks, which are attributed to the electron-light hole (higher energy) and heavy hole (lower energy) transition, respectively. This is an important feature of 2D NPLs commonly observed in the absorption spectrum. Moreover, two high-intensity exciton absorption peaks at room temperature indicate the larger exciton binding energy. Compared with CdSe QDs and bulk materials, the huge anisotropy and strong 1D quantum confinement of 2D NPLs lead a big increase of exciton binding energy. Due to the different thickness of the NPLs and the dielectric constant of the surrounding environment, the exciton binding energy varies from 100 to 400 meV in early reasearch.[53] Similar result was reported by many other

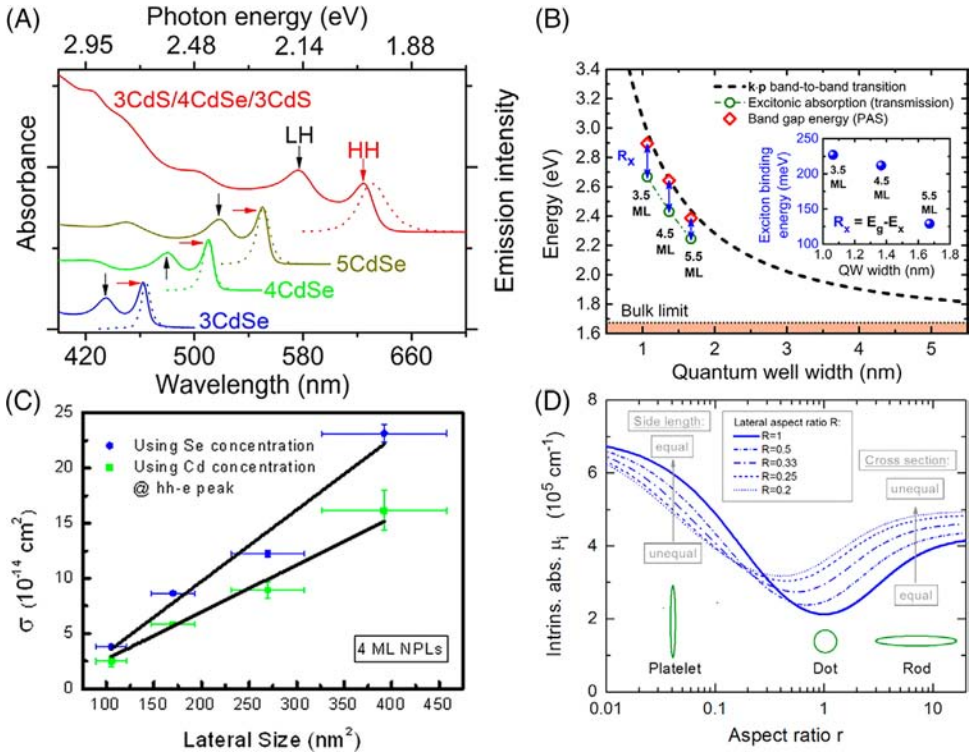

FIGURE 1 A, Absorption (solid lines) and PL (dashed lines) spectra of CdSe NPLs with 3, 4, 5 monolayers. Copyright © 2015 American Chemical Society. B, Excitonic absorption in room-temperature optical transmission (green circles), and the fundamental band gaps determined from the photoacoustic spectra (red boxes). The inset shows the exciton binding energy of CdSe NPLs as a function of thickness, which is determined by the difference between the two data above. Copyright © 2019 American Chemical Society. C, Lateral size dependence of the absorption cross-section at the energy of heavy-hole to electron transition of 4 MLs CdSe NPLs. Copyright © 2015 American Chemical Society. D, Aspect ratio dependence of the intrinsic absorption coefficient for CdSe system. Copyright © 2015 American Chemical Society. NPLs, nanoplatelets; PL, photoluminescence

researches.[54-56] Recently, Zelewski et al use the combination of optical and photoacoustic spectroscopies to characterize exciton binding energy of CdSe NPLs with thickness from 3 to 5 MLs.[57] The exciton binding energy is calculated from the difference between the lowest excitonic transition taken from standard spectrometric measurement (optical transmission) and the band gap energy obtained from the photoacoustic spectrum. The determined exciton binding energy for CdSe NPLs ranges from 130 to 230 meV, which depends on the thickness as shown in Figure 1B. The large exciton binding energy of the CdSe NPLs ensures the stable exciton at room temperature, which is an important factor for high-efficiency light emission.

Due to the strong 1D confinement, NPLs have been predicted to possess a giant oscillator strength transition (GOST), which lead to an enhancement of the absorption cross-section.[22] Later, Tessier et al evaluated the absorption cross-section of NPLs at 400 nm in hexane to be ~2.5×10^{-13} cm^2, about 1 order of magnitude larger than a spherical QDs with the same emission wavelength.[58,59] As an important parameter for optical materials, the absorption cross-section is an important indicator for practical application. She et al has pointed out that the large absorption cross-section of CdSe NPLs is one of the reasons for the large optical gain. In addition, the growth of the CdS shell further increases the absorption cross-section, thus achieving a lower ASE threshold.[60] In 2015, Yeltik et al experimentally determined the absorption cross-section of CdSe NPLs. As shown in Figure 1C, the absorption cross-section is strongly related to the lateral size.[61] The shape-dependent linear absorption properties were studied by Achtstein et al in the same year.[62] They used the volume-independent intrinsic absorption coefficient, which given by dividing the absorption cross-section by the volume of the nanocrystals. The aspect ratio dependence of the intrinsic absorption coefficient is shown in Figure 1D. It can be observed that the high aspect ratio of the NPLs leads to a higher intrinsic absorption coefficient compared to spherical QDs and nanorod. In addition to these parameters, the thickness of NPLs can also affect the intrinsic absorption

coefficient.[43] The 2 MLs NPLs show a larger intrinsic absorption coefficient than thicker NPLs. All these studies show that the NPLs is an outstanding optical material with strong absorption, which makes them ideal for applications such as light harvesting devices and lasers.

The PL of the NPLs showed a marked difference compared with spherical QDs and nanorods. The PL spectrum of CdSe NPLs is shown in Figure 2A, which presents a very narrow FWHM. This special optical feature is induced by the 2D structure of the NPLs. The exciton Bohr radius of the CdSe NPLs is considered to be around 3.5 to 4 nm.[53,58] Generally, the synthesized NPLs have a lateral dimension of about 10 to 100 nm, excitons have not been strongly confined at this scale. Therefore, the CdSe NPLs only exhibit quantum confinement in the thickness direction. At the same time, all the NPLs in solution have the same thickness at the level of atomic layer. Different from QDs, the size distribution of the NPLs in the lateral dimensions does not affect their transition energies, and therefore shows a small FWHM. After the elimination of inhomogeneous broadening, the FWHM of the NPLs is usually around 30 to 50 meV (7-10 nm), which is smaller than QDs.[22] The emission line of the NPLs can be well-fitted with Lorentzian rather than Gaussian, which proves the disappearance of inhomogeneous broadening.[41]

It is interesting to find that the CdSe NPLs also show different PL spectra at low temperature. There have two emission peaks with a small energy difference appeared at low temperature. However, one can find many different explanations for the origin of low-energy peak. Tessier et al believe that the low-energy peak is a phonon line induced by the stacked CdSe NPLs in 2013.[63] The energy difference between the two peaks is 25 meV, which is very close to the longitudinal optical (LO) phonon energy of the CdSe bulk semiconductor. However, it was found in the experiment that the low-energy peak was not observed at a single nanoplatelet at low temperature, and the intensity of the low-energy peak was related to the excited area of the sample. They proposed a model of stacked NPLs to explain the generation of low-energy peaks. Because the free exciton emission of the NPLs has a very small stokes shift, the stacked NPLs will lead to a strong reabsorption, while the low-energy phonon peaks can avoid being reabsorbed. Therefore, free exciton peaks are continuously reabsorbed and

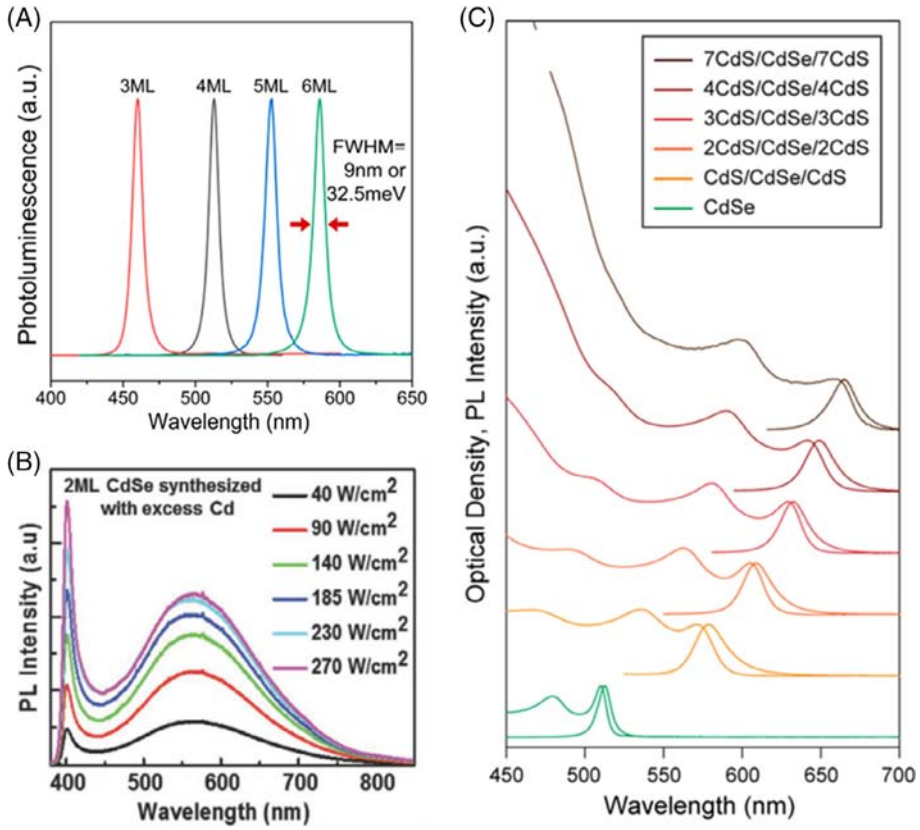

FIGURE 2 A, PL spectra of CdSe NPLs with different thickness from 3 to 6 MLs. Copyright © 2018 American Chemical Society. B, PL spectra of 2 MLs CdSe NPLs at different excitation power. Copyright © 2019 WILEY-VCH Verlag GmbH & Co. KGaA, Weinheim. C. Absorption and PL spectra of CdSe/CdS core/shell NPLs with different shell thickness. Copyright © 2012 American Chemical Society. NPLs, nanoplatelets; PL, photoluminescence

stronger phonon peaks are generated. In 2006, Achtstein et al proposed that the two peaks were attributed to s- and p-exciton state. Moreover, it was found in experiments that the energy difference between the two peaks is related to the lateral size of the CdSe NPLs, ranging from 19 to 38 meV.[64] The charged exciton origin of low-energy peak was reported by Shornikova et al in 2018. They found that the energy separation between two peaks changes with NPL thickness, which is different from the LO phono energy of CdSe. In addition, the external magnetic field has different effects on the PL decay and intensity of these two peaks. The low-energy peak shows typical feature for charged excitons with a bright ground state.[65] Later, the low-energy peak was assigned to excimer-like emission by Diroll et al.[66] The stacked NPLs form an excimer-like structure and inter-NPL interactions leads to a low-energy emission. The low-energy peak shows strong sensitivity to pressure, concentration of NPLs, and self-assembly into stacks, which are the obvious feature of excimer emission in molecular fluorophores. Recently, we have proposed new insights into the origin of low-energy peak of CdSe NPLs.[67] The low-energy peak is originated from surface state-related emission. Continuous laser irradiation increases the number of surface states of the sample, resulting in a decrease of the free exciton emission and an increase of the surface state-related emission. In addition, the intensity of low-energy peak is related with the lateral size of CdSe NPLs. The surface passivation treatment can significantly reduce the proportion of low-energy peak. The unique 2D structure makes the NPLs have a larger surface area to volume ratio, which is an important parameter that affects their optical properties.

The emission wavelength of CdSe NPLs is only determined by the thickness. One can only increase or decrease by number of atomic layers, therefore the CdSe NPLs generally has fixed emission wavelengths corresponding to the number of layers. For commonly used CdSe NPLs with 3, 4, 5, 6 MLs, the corresponding emission wavelengths are about 462, 513, 553, and 585 nm, as shown in Figure 2A.[68] When the thickness of the CdSe NPLs decrease to the sub-nanometer scale (2 MLs), the surface defects will lead to intensive surface emission.[43] As shown in Figure 2B, the PL spectrum of 2 MLs CdSe NPLs shows a narrow emission at 405 nm, which is the band edge excitonic emission. In addition, a big broad emission appears at 550 nm, which is the radiative recombination through surface emission centers. The surface state in the 2 MLs CdSe NPLs is believed to be the localized holes at unpassivated Se sites. The effect of surface on emission is more obvious in thinner NPLs. Similar PL spectra also appears in 3 MLs CdSe NPLs.[40,50] In recent years, by adding chlorides during the growth process, the synthesis of 6 to 8 MLs NPLs can be achieved, covering the red emission band.[45,68]

Controlling the emission wavelength of NPLs by thickness sometimes cannot meet the requirements of research and application, and its QY and photostability also need to be further improved. Therefore, many methods are proposed to obtain NPLs with higher efficiency, wider emission wavelength coverage, and better stability. Semiconductor heterostructures have been widely used as a method of tuning the emission properties, and there have been many related studies in CdSe NPLs. As mentioned before, core-shell CdSe NPLs structure are the earliest NPLs heterostructure.[25,46] The single-layer controllable growth of the CdS shell was achieved by the c-ALD method at room temperature.[25] The PL spectra of CdSe/CdS core/shell NPLs with different shell thickness is shown in Figure 2C. The emission peaks red-shift from 510 to 665 nm with the increase of shell thickness. The growth of the CdS shell changes the spatial distribution of the electron and holes in the CdSe NPLs. The holes are still confined in CdSe core, while the electrons will gradually delocalize into the CdS shell, which cause the red shift of the emission peak. In addition, the growth of the shell will lead to the increase of FWHM.[69] It can be seen from the Figure 2C that after the shell grows, the FWHM increases. However, this is not due to inhomogeneous broadening caused by emission of different individual NPLs. Because the PL spectra of single core/shell NPLs show a comparable FWHM with the ensembles. Researchers believe that this broadening is due to the enhanced coupling of excitons and phonons.[69] The electrons delocalized into the CdS shell layer will lead to interact between excitons and phonons in CdS, thus increasing the exciton phonon coupling. CdSe/ZnS core/shell NPLs with Type-I band alignment was synthesized at moderate temperature (100°C-150°C), and its QY was improved compared to CdSe core.[70] The high-quality CdSe/ZnS core/shell NPLs can be synthesized through hot-injection shell growth.[47] Compared with the shell synthesized at a lower temperature, the ZnS shell synthesized at 300°C has a higher crystal quality, which makes this core/shell NPLs have a QY of up to 98% and excellent thermal stability. Moreover, by synthesizing the alloyed shell, the lattice mismatch between the core and shell can be improved. The optical performance of the NPLs can be further improved, and a low threshold ASE is successfully realized.[36] Recently, core/shell NPLs with various shell designs have been achieved through a slow-injection shell-growth method. A compositionally graded alloyed shell further optimized the optical properties of the NPLs.[37]

Compared with the core-shell structure, the core-crown structure in the NPLs heterostructure can achieve

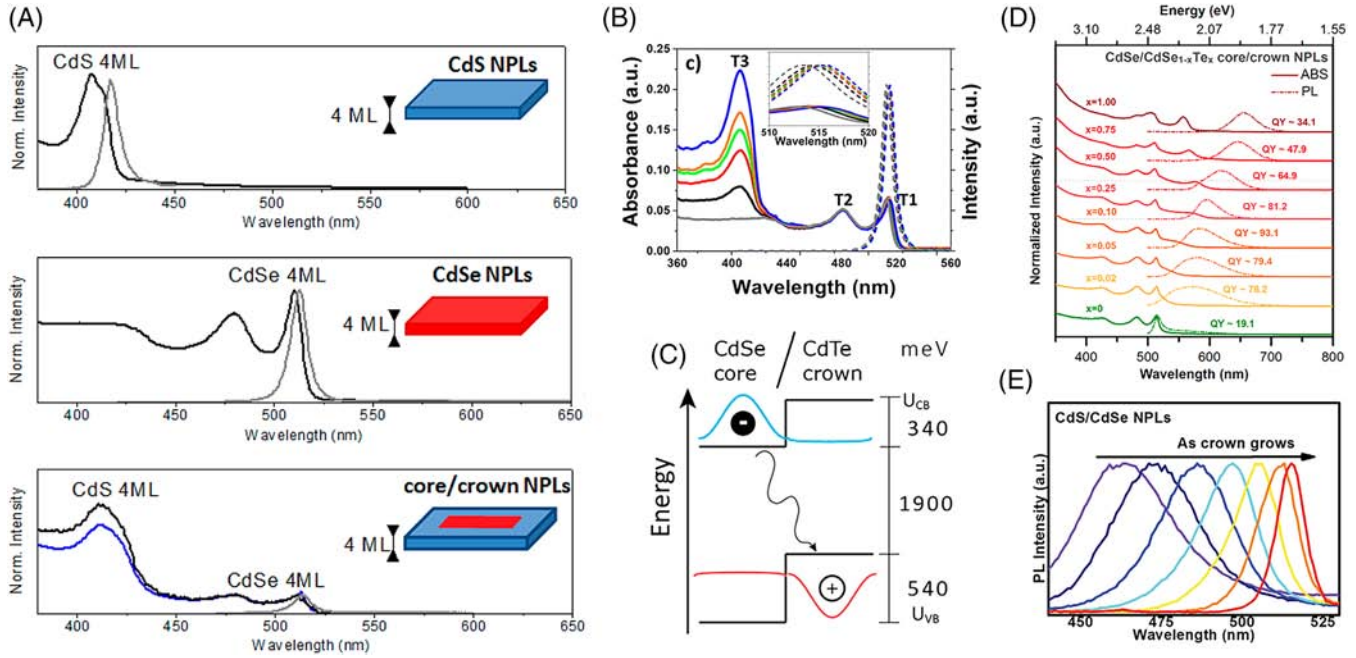

FIGURE 3 A, Absorption (black) and PL (gray) spectra of CdS, CdSe, and CdSe/CdS core/crown NPLs. Copyright © 2014 American Chemical Society. B, Absorption (solid line) and PL (dashed line) spectra of CdSe/CdS core/crown NPLs with different crown sizes. From gray to blue line, the size of crown gradually increases. Copyright © 2016 American Chemical Society. C, Band alignment in Type-II CdSe/CdTe core/crown NPLs. The electrons are confined in the CdSe core, while the holes are confined in the CdTe crown. Copyright © 2014 American Chemical Society. D, Absorption (solid line) and PL (dashed line) spectra as a function of crown composition. Copyright © 2017 American Chemical Society. E, PL spectra of inverted Type-I CdS/CdSe core/crown NPLs with different crown size. Copyright © 2015 WILEY-VCH Verlag GmbH & Co. KGaA, Weinheim. C. NPLs, nanoplatelets; PL, photoluminescence

the optimization of optical properties without changing its emission wavelength. As shown in Figure 3A, the growth of the crown induced a significant CdS absorption band in the absorption spectrum, but the emission peak position did not shift significantly.[28] As the crown expands, the NPLs show stronger absorption feature of CdS crown as shown in Figure 3B.[71] In these core/crown structures, excitons collected by the CdS crown are transferred rapidly to the CdSe core, the crown can be used as an effective optical antenna. By changing the material of the crown, a core/crown NPLs with a type-II band structure can be obtained.[48,72,73] In this type-II structure, all electrons are localized in the CdSe core, and all holes are localized in the CdTe crown. The excitons recombine near the interface between core and crown, leading a significantly red-shift of the emission peak, as shown in Figure 3C. Through precise composition design of the type-II NPLs heterostructure, the CdSe/$CdSe_{1-x}Te_x$ NPLs achieves a wider range of adjustable emission wavelengths as shown in Figure 3D.[74-76] Moreover, at a certain composition, the QY of the NPLs can be improved up to 95% due to the suppression of nonradiative hole trap sites.[75] In addition to these, the behavior of tunable wavelengths can be achieved by the synthesis of inverted type-I CdS/CdSe core/crown NPLs heterostructures.[49] In this structure, CdS NPLs with a wider band gap is used as the core, and then CdSe with a narrower band gap continues grown as crown. When the lateral size of the CdSe crown is large enough, the quantum confinement effect only occurs in the thickness direction. Therefore, without changing the thickness, the emission wavelength of the NPLs will not shift. However, when the CdSe crown started to grow, its lateral size was small enough to generate a stronger quantum confinement than the thickness direction, so the emission peak would be significantly blue-shifted. Therefore, by controlling the size of the CdSe crown, continuous tunable emission from CdS NPLs (421 nm) to CdSe NPLs (515 nm) can be achieved, as shown in Figure 3E. In addition to these simple NPLs heterostructures, some complex structures have emerged. Through layer by layer growth, a composition-tuned gradient $Cd_{1-x}Zn_xS$ shell cover on the CdSe/CdS core/crown seeds.[29] The periphery and surface of CdSe NPLs are better passivated, and the surface is capped with dense ligands, thus achieving high QY in aqueous solution.

For optical property modification, doping has been used in bulk semiconductor and QDs materials. Introducing metal ions into the crystal lattice of semiconductor nanocrystals will generate new energy levels, which will induce changes in the emission properties. A variety of

metal ions have also been successfully doped in NPLs. When CdSe NPLs were doped with Mn^{2+}, it was found that a strong Mn^{2+} emission occurred at about 590 nm. Meanwhile, the emission of CdSe has been substantially suppressed at about 460 nm, as shown in Figure 4A.[77] The Cu^{2+} also can be doped in CdSe NPLs.[50,52,78] Figure 4B shows the absorption and PL spectra of Cu-doped CdSe NPLs with different thickness. It can be seen that the introduction of Cu^{2+} does not have any effect on the original absorption of the CdSe NPLs, while the emission is dominated by a red-shifted broadband. The band diagram is shown in Figure 4C. The doping of Cu^{2+} generates a mid-gap, which results in the red emission. By controlling the amount of Ag^{2+} doped in the CdSe NPLs, continuous adjustment of the emission color from green to red can be achieved.[79,80] Figure 4D,E show the emission of the CdSe NPLs with different amount of dopants. Recently, mercury ions have also been doped into CdSe NPLs.[51] At different doping temperatures, the presence of mercury ions in the NPLs lattice is also different. At lower temperature doping, mercury atoms may replace cadmium atoms, or they may just interstitial incorporated, thus causing dual emission peaks. However, at high temperature doping, the mercury atoms completely replace the cadmium atoms, so there is only a single emission peak.

In addition to the metal ion doping, the anion doping can also tune the emission properties of the CdSe NPLs. By introducing mixtures of Se and S powders with different proportions as anion sources during the synthesis process, the alloyed $CdSe_xS_{1-x}$ NPLs was successfully implemented. With the increase of the ratio of S component, the thickness of the NPLs will not change, while the emission peak shows a significant blue shift.[34,81] It is well-known that surface ligands have a great influence on the optical properties of semiconductor nanomaterials. For CdSe NPLs, ligand exchange has also been found effective to modify the emission properties. In 2017,

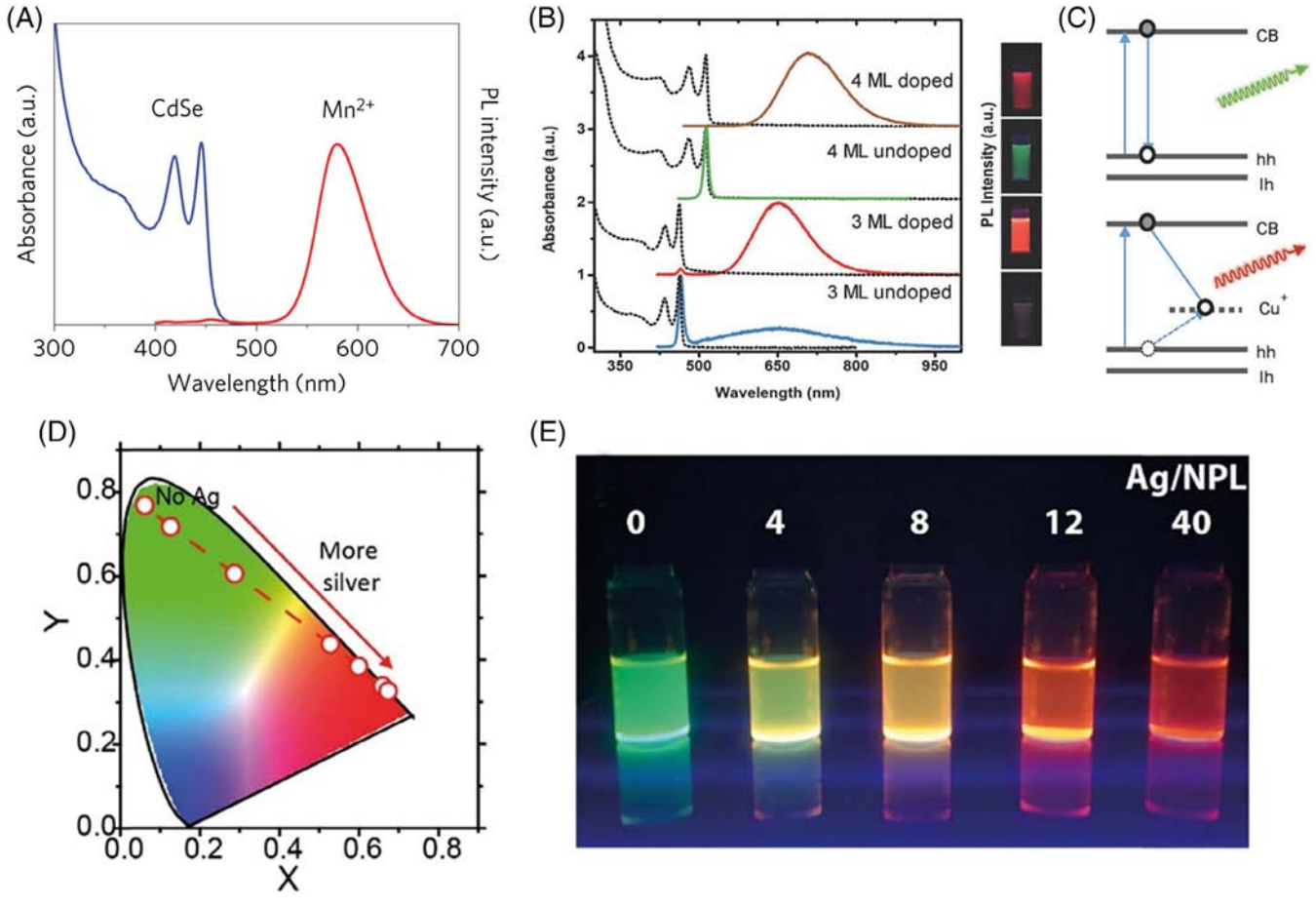

FIGURE 4 A, The absorption (blue line) and PL (red line) spectra of Mn-doped CdSe NPLs. Copyright © 2009 Springer Nature. B, Absorption (dashed line) and PL (solid line) spectra of 3 and 4 MLs Cu-doped and undoped CdSe NPLs. C, Energy band diagram of Cu-doped and undoped CdSe NPLs. B,C, Copyright © 2017 WILEY-VCH Verlag GmbH & Co. KGaA, Weinheim. D, Different color with increasing doping amount of Ag on the chromaticity diagram shows. E, Image of CdSe NPLs solution with different amount of Ag doped. D,E, Copyright © 2019 American Chemical Society. NPLs, nanoplatelets; PL, photoluminescence

Antanovich et al replaced the native oleic acid ligand with aliphatic thiol or phosphonic acid on the surface of CdSe NPLs, which resulted in a large red-shift (up to 240 meV) of emission peak. However, this ligand exchange causes larger PL quenching.[82] In 2019, Dufour et al found that using of halide ligands can tune the emission properties and significantly improve PLQY.[83] The red shift leaded by ligand exchange is mainly considered to have two reasons. First, ligand exchange releases the internal stress of the NPLs, which leads to expansion of the crystal lattice in the thickness direction. Second, the delocalization of wave function over the surface ligands weakens the confinement.

3.2 | Carrier dynamics

PL spectroscopy is a steady-state measurement technique commonly used to study the optical properties of semiconductors. Information such as emission intensity and wavelength can be obtained from the PL spectrum. However, time-domain information of the material cannot be studied by the method mentioned above. It is known that after laser excitation, the carriers inside semiconductor material are excited, and then a series of processes occur, such as carrier cooling, relaxation to the band edge, trapping, and radiative recombination. The carrier dynamics in the semiconductor material greatly affects the emission characteristics. Therefore, in order to improve the optical properties of semiconductor materials, it is necessary to have an in-depth understanding of its carrier dynamics. In recent years, there have been some studies on the carrier dynamics of CdSe NPLs.

Through time-resolved PL measurement, the carrier relaxation process of CdSe NPLs was studied. Figure 5A shows the PL spectra of CdSe NPLs in different time scales after excitation. An exponential tail on the high-energy side of the PL spectrum appears, which corresponds to recombination of higher-energy carriers.[84] After excitation, the internal carriers reach thermal equilibrium within a very short time. Subsequently, the hot carriers begin to gradually cool to room temperature, which can be seen from the gradually disappeared-tail. The temperature of the carriers can be estimated by fitting the high-energy emission tail generated after laser excitation. The carrier temperature as a function of time after excitation is shown in Figure 5B. It can be seen that the carrier temperature has a very rapid decrease at the beginning. After a rapid decay of several tens of picoseconds, the temperature of the carrier decreases to room temperature.[85] However, in another study, this rapid decay process was reported in only a few picoseconds,

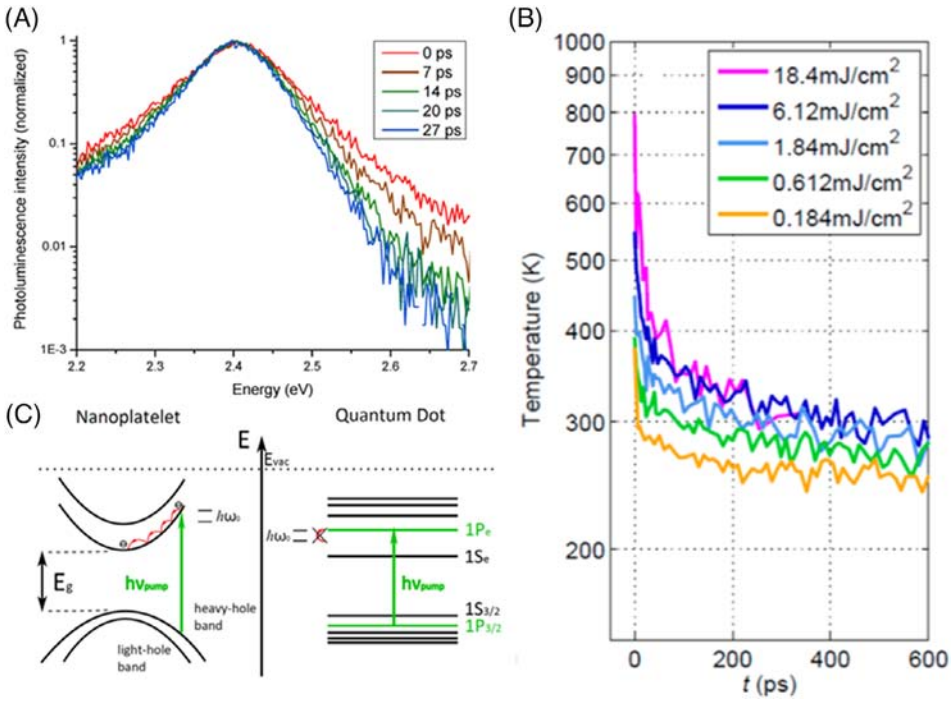

FIGURE 5 A, PL spectra of 6 MLs CdSe NPLs at different times after excited by an ultrafast laser pulse. The spectra are normalized by the maximum value. Copyright © 2012 American Chemical Society. B, Carrier temperature as a function of time after excitation at different pump intensity. Copyright © 2015 American Chemical Society. C, The different electron relaxation process in NPLs and QDs. Copyright © 2015 American Chemical Society. NPLs, nanoplatelets; PL, photoluminescence

which is thought to be caused by different excitation intensities.[86] The CdSe NPLs show a significantly higher carrier energy loss rate than CdSe QDs. This difference in carrier cooling rate can be explained by different band structures. As shown in Figure 5C, since the CdSe NPLs has quantum confinement only in one dimension, it has a continuous density of states. After the electrons are excited to high energy, it begins to interact with phonons. By transferring the energy to the LO phonon, the electrons relax to the lowest energy position in the conduction band. However, for QDs, the energy difference between the energy levels of the electrons is greater than the phonon energy, so the pathway to relax by emitting a single phonon is suppressed. This phenomenon is called the phonon bottleneck effect in QDs.[87] The carrier cooling process is a slow decay, which is considered to be caused by the hot phonon bottleneck effect.[86] Carriers that are rapidly cooled at the beginning produce a large number of phonons. These phonons did not have enough time to diffuse and then reabsorbed by the carriers, resulting in a slower carrier temperature drop rate. In addition, it was found that the thickness of CdSe NPLs or the CdS Shell did not markedly influence the cooling kinetics.[86]

The decay pathways of photoexcited states in CdSe and CdSe/CdS NPLs have been studied by Kunneman et al. The PL decay dynamics of CdSe NPLs were found to be nonexponential.[53,58,69] It means that during the exciton decay, there are other pathways besides the direct recombination to the ground state. By comparing the PL decay with transient absorption (TA) data, it is believed that exciton quenching site exists in a fraction of CdSe platelets.[88] The bleach signal of the heavy hole transition to conduction band in the TA decays much slower than the PL decay. Exciton quenching results in excess electron or hole in the NPLs, which can be clearly observed in the bleach signal. The rate of charge transfer from the exciton to the quenching sites is much faster than the rate of exciton recombination to the ground state. Therefore, after the generation of excitons due to excitation, most of the excitons are quenched within a few hundred picoseconds. This is mainly shown in the initial fast decay part of PL decay. Subsequently, the exciton recombination to the ground state dominates by a slower decay process. In addition, once the holes are trapped, the electrons in the conduction band are not free to move, but will be localized by the influence of huge exciton binding energy.

In addition to picosecond and nanosecond carrier dynamics, the microsecond dynamics has also been noticed in CdSe NPLs.[89] In addition to the rapid radiative and nonradiative recombination process, there is a phenomenon called delayed emission up to microsecond in CdSe NPLs. By fitting the PL decay process, the delayed emission contributes more than 50% of the total emission of CdSe NPLs. In QDs, the proportion of such delayed emission is only about 10% to 25%.[90] The emission line with a delay of a few microseconds has the same shape as the initial spectrum, which proves that the excitonic properties have not changed. This phenomenon is considered to be the process of temporary charge carrier trapping, then the trapped charge release and return to emission.

The delayed emission phenomenon was also found in the CdSe/CdS core/shell and core/crown structure. The coating of the shell or crown reduces the defect state and achieves a higher QY, but the delayed emission has not been changed compared to the CdSe core. This proves that the temporary trapping is not directly related to PL quenching. Because the quantum confinement only exists in the thickness direction of the NPLs, excitons can move freely within the plane. A depth understanding of exciton and carrier transport processes in NPLs is of great significance for some optoelectronic applications, such as light harvesting and photocatalysis. The NPLs heterostructure is a suitable platform for studying carrier transport processes. The charge carrier transport caused by the band offset of two materials can be recorded and analyzed by TA spectroscopy. The exciton localization efficiency and localization time in CdSe/CdS core/crown NPLs have been studied.[71] In the TA measurement, the state-filling of the conduction band electron level cause the exciton bleach signals in CdSe and CdS rather than the hole in the valence band.[91] Thus, the conduction band electron dynamics can be detected through TA measurement. The CdSe/CdS core/crown NPLs show a type-I band alignment. After optical excitation, excitons in the CdS crown are rapidly transported to the CdSe core. The exciton localization time is less than 1 ps and will increase as the crown size increases. The TA spectrum is shown in Figure 6B, where CdSe/CdS core/crown NPLs was excited by 400 nm pump laser. T3 corresponds to the electron transition in the CdS crown as shown in Figure 6A. Normalized T3 bleach kinetics of five samples with different crown size is shown in Figure 6C, and the crown size gradually increases from CC1 to CC5. It can be seen that as the crown size decreases, T3 bleach signal has a faster decay rate. The decay of T3 bleach signal represents that electrons are transport from the conduction band of CdS to the conduction band of CdSe, so it can be found that a CdSe/CdS core/crown NPLs with a small size crown has a shorter exciton local time. This phenomenon of crown-related exciton local time is also reported in the CdSe/CdTe core/crown NPLs structure.[92] However, the local efficiency of the exciton is not affected by the size of the crown. This is because the holes are

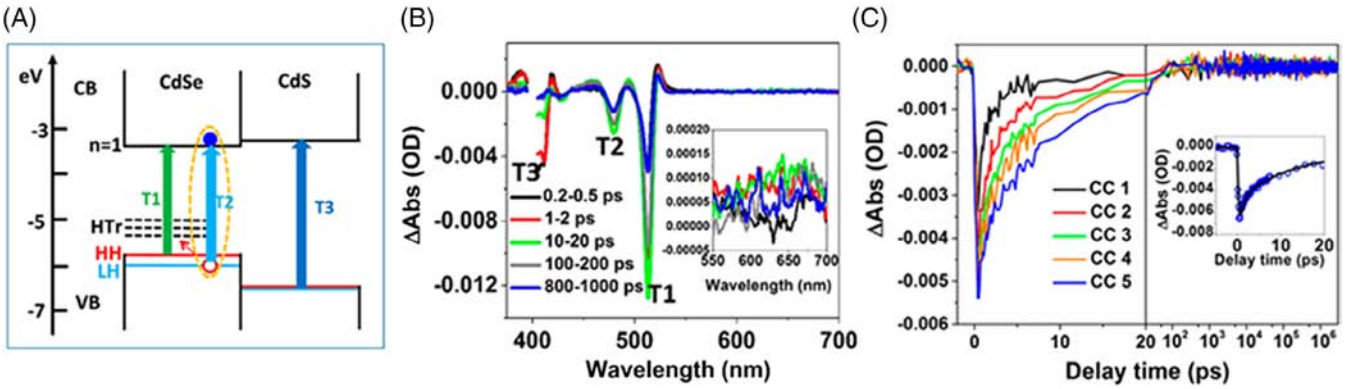

FIGURE 6 A, Band alignment of CdSe/CdS core/crown NPLs. HH and LH represent heavy holes and light holes, respectively. The HTr are hole trapping state. B, TA spectra of CdSe/CdS core/crown NPLs at different time after the excitation of 400 nm laser. C, Normalized bleach signal of electron transition in CdS crown (T3). A,B,C, Copyright © 2016 American Chemical Society. NPLs, nanoplatelets

trapped at the interface between CdSe and CdS, and the size of the crown does not affect the state of traps at the interface.[71] Similar results for exciton and carrier transport of CdSe/CdS core/crown NPLs have also appeared in type-II NPLs heterostructures, such as CdSe/CdTe and CdS/ZnSe core/crown NPLs.[92-94] Moreover, these type-II NPLs heterostructures exhibit long-lived charge transfer exciton state, about 30 times longer than core-only NPLs.[93,94] These longer lifetimes are thought to be the result of the spatial separation of electrons and holes. Recently, more detailed charge transfer dynamics in CdSe/CdTe core/crown NPLs have been reported.[95] The generation of charge transfer excitons involves two processes. The first process is the ultrafast electron transfer (~70 fs), and then the charge carriers diffuse through the CdSe and CdTe (~5 ps).

3.3 | Optical gain and nonlinear optical properties

Since stimulated emission was first observed in colloidal QDs in 2010, it has been widely considered as a promising gain material.[16] The superior lasing performance and low-cost solution processability make it suitable for integration into various optoelectronic device platforms. Compared to QDs, NPLs have larger absorption cross-sections, narrower light emission, and longer multiexciton lifetimes, which make it better optical gain materials.[96-98]

ASE was observed in CdSe NPLs in 2014. The ultralow threshold of 6 μJ/cm^2 was achieved under the pumping of femtosecond laser at room temperature.[55] This ASE threshold is lower than many optimized CdSe QDs and nanorod structures. It is considered that the optical gain in NPLs comes from the stimulated emission of biexciton states.[99] Multiexciton recombination is mainly affected by Auger recombination. Electrons and holes recombine nonradiatively and transfer energy to another electron or hole to fulfill momentum and energy conservation. The large Auger recombination rate causes the multi-exciton population to decay rapidly, which will greatly increase the threshold of optical gain. Strong Auger recombination hinders the further development of QDs as optical gain materials.[100,101] Compared with QDs, the Auger recombination process in NPLs is suppressed due to strict momentum conservation constraints. Auger becomes more complicated in higher-dimensional systems.[97] The Auger lifetime of the CdSe NPLs measured in the experiment is much longer than that of QDs with the similar emission wavelength, which reaching 500 ps.[60] In another work, it was shown that the biexcitons Auger recombination rate in the CdSe NPLs is about 1 order of magnitude lower than CdSe QDs and nanorods.[97] In addition, CdSe NPLs have been reported to have high biexciton quantum yields, which is important for achieving ASE with lower threshold.[102] Gain bandwidth and gain lifetime are also important parameters for evaluating an optical gain material. These parameters can be obtained from the absorption measurement combined with TA measurement. The absorption spectra (α_0) and transient spectrum (α) are shown in Figure 7A. The α is calculated from $\alpha_0 + \Delta\alpha$, where $\Delta\alpha$ is measured from the TA. The optical gain is indicated by the red area where $\alpha < 0$. It can be seen that the gain occurs from 590 to 660 nm, which demonstrates a large gain bandwidth. The dynamics of optical gain are shown in Figure 7B. CdSe NPLs show a gain lifetime of 140 ps, which is longer than those QDs and nanorods.[103-105] Modal gain coefficient is another key parameter for the optical gain material. A high gain coefficient means that the optical gain can overcome the loss caused by the material itself to obtain optical amplification within a

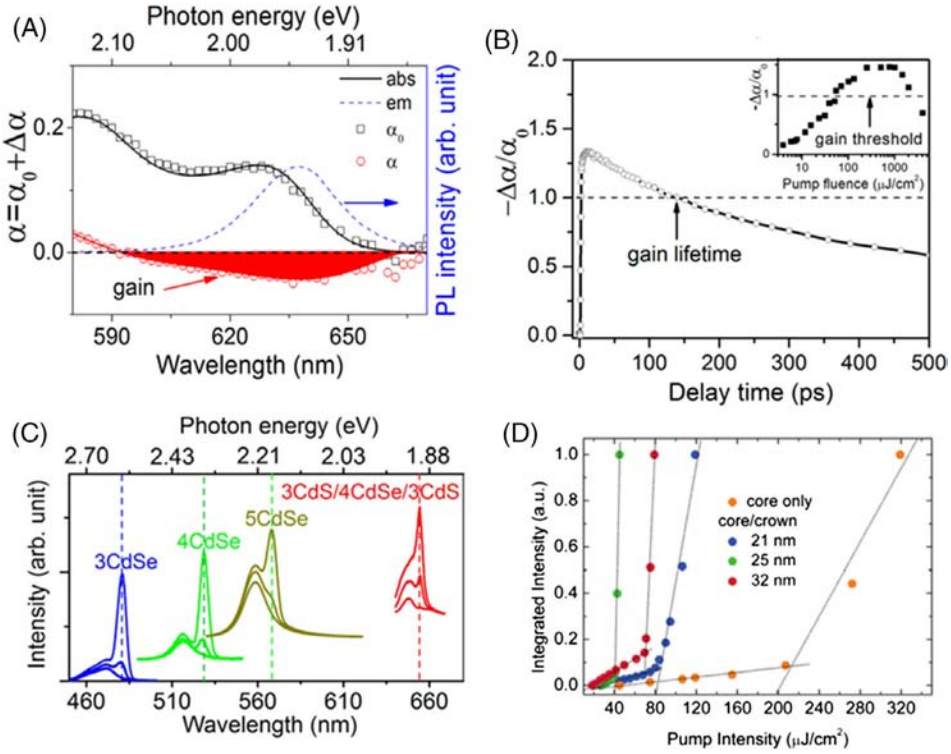

FIGURE 7 A, Absorption (α_0), PL, and transient spectra ($\alpha = \alpha_0 + \Delta\alpha$) of CdSe/CdS core/shell NPLs. B, Optical gain dynamics monitored at 644 nm for CdSe/CdS core/shell NPLs. C, Lasing with different color realized by tuning the thickness of CdSe NPLs and heterostructure. A,B,C, Copyright © 2015 American Chemical Society. D, Integrated PL intensity as a function of pump intensity with core only CdSe NPLs and CdSe/CdS core/crown NPLs. Copyright © 2014 American Chemical Society. NPLs, nanoplatelets; PL, photoluminescence

shorter gain length. The gain coefficient is usually measured through the variable stripe length (VSL) method.[106] The gain coefficient of CdSe NPLs has been reported in many works, ranging from 600 to 930 cm^{-1}.[35,60,103,107] Due to the longer gain lifetime and suppressed Auger recombination of CdSe NPLs, it exhibits larger gain coefficient than CdSe QDs and nanorods. In addition, even under intensive pumping that exceeds the gain threshold by two orders of magnitude, the CdSe NPLs can sustain large gain. However, since multiple excitons cannot be supported on the band edge in QDs, the gain coefficients saturate when the pump intensity reaches approximately twice of the threshold.[108]

The PL properties of CdSe NPLs can be controlled by changing the lateral size, thickness, and heterostructure. Those methods can also affect the optical gain of CdSe NPLs. The emission wavelength can be tuned by changing the thickness of CdSe NPLs. Combined with the advantage of high optical gain, the blue ASE can be achieved from the 3 MLs CdSe NPLs. Moreover, the green, yellow, and red ASE can also be obtained thorough CdSe NPLs with different thickness, as shown in Figure 7C.[103] Although the thickness of the NPLs lead a strong quantum confinement, the lateral size of the NPLs can also affect the exciton movement in plane, and then change the properties of optical gain. The ASE threshold was found to increase obviously with the increase of the lateral size. It is believed that larger NPLs have more nonradiative recombination centers due to defects, thereby reducing the optical gain threshold.[109] However, the biexciton Auger lifetime and biexciton quantum yield have been reported to increase with increasing lateral size, which will be helpful for the reduction of the threshold.[96,102] In addition, some works suggest that the optical gain threshold is independent of the lateral size, only the saturation optical gain increase with the lateral size.[99,103] Here, due to the different synthesis quality of the NPLs, the optical gain is a complicated process with many influencing factors. The effect of lateral size on the optical gain of NPLs needs more comprehensive research.

The optical gain of CdSe NPLs can also be optimized through heterostructures. As shown in Figure 7D, all of the core/crown NPLs shows a smaller ASE threshold than the core-only NPLs.[35] Comparing NPLs with different crown sizes, it was found that the NPLs with medium-sized crowns have the lowest ASE threshold. The CdS crown acts as an exciton concentrator, which increases the absorption cross-section and reduces the

ASE threshold. However, the increase of the crown size may bring more defects, which leads to the quenching of excitons and the increase of ASE threshold. In the type-II heterostructure, electrons and holes are spatially separated, where the small wave functions overlap and suppress Auger recombination. Therefore, the type-II heterostructures are considered to be promising gain materials. The type-II CdSe/CdTe core/crown NPLs have been reported to show a low ASE threshold.[110] Because of the spatial separation of core and crown exciton, the multiple exciton states show a long lifetime compared to QDs. The alloyed CdSe/CdSeTe crown can reduce the number of the defects and increase the Auger recombination lifetime, which enables a large optical gain.[111] In addition, tuning the composition of the alloyed crown can achieve optimal optical gain and achieve tunable ASE wavelength.[30,106] Recently, core/shell NPLs with better stability and optical properties were obtained through some novel synthesis methods.[36,37] An record-low ASE threshold of 2.4 $\mu J/cm^2$ has been achieved using the core/shell CdSe/CdZnS NPLs, which were synthesized through hot-injection method.[36]

Multiphoton absorption is a valuable optical nonlinear property in semiconductor nanocrystals. By absorbing multiple low-energy photons, the electrons are excited to the conduction band, and then recombine to emit a high-energy photon. Because it can convert widely used low-energy photons in biology to high-energy photons in the visible range, multiphoton absorption has important applications in biological fields.[112,113] The NPLs show excellent multiphoton absorption characteristics. Two-photon and even three-photon pumped ASE have been demonstrated with low thresholds ranging from 0.5 to 4.5 mJ/cm^2.[30,35,36,109,114] The two-photon absorption cross-section of CdSe NPLs is about 10^5 GM measured by Z-scan, which is an order of magnitude larger than the highest two-photon absorption cross-section in QDs.[109,115] In addition, the two-photon absorption cross-section of CdSe NPLs show a volume dependent.[116] Large volume NPLs will have larger two-photon absorption cross-section.

3.4 | Stacking of nanoplatelets

The unique anisotropic 2D shape of the NPLs make them easy to stack together. NPLs are connected to each other through two large surfaces to form a stacked structure. Such stacked NPLs assemblies have been shown to exhibit different optical properties compared with non-stacked one. When ethanol is added to the NPLs solution, the NPLs tend to escape from ethanol to minimize their surface energy, because ethanol is an anti-solvent for oleic acid ligands. Therefore, the addition of ethanol can induce the stacking of NPLs. Figure 8A,B show the TEM image of the NPLs with 0 and 455 μL ethanol. The addition of a large amount of ethanol significantly exacerbated the stacking of NPLs. As shown in Figure 8C, with the increase of the amount of ethanol added, the PL quenching become more significant.[31] The emission wavelength and FWHM did not change significantly in this process. It is believed that Förster resonance energy transfer (FRET) occurs in the stacked NPLs. Excitons are transported between different NPLs. Nonradiative recombination occurs when a defective or non-emissive NPLs is encountered, and this causes a strong PL quenching.[31,32] In QDs, FRET causes the red shift of the emission wavelength, due to the non-uniformity of its size.[117] However, the precise thickness makes the phenomenon of red shift disappear during the FRET process of the NPLs. The NPLs have been reported to form micrometers long needle-like superparticles by self-stacking, as shown in Figure 8D.[118] The NPLs are stacked together to form a highly aligned columnar structure, whose main axis is perpendicular to the plane of the NPLs. These ordered NPLs structures lead to an anisotropic optical property, and obvious polarization emission characteristics have been found in experiment as shown in Figure 8E,F. In addition, electronic transport in stacked CdSe NPLs based polymer fibers have been reported.[81] This structure may find applications in many optoelectronic devices. In addition to stacking of NPLs from same population, the FRET process of stacked NPLs of different thicknesses has also been studied.[119] When the donor's emission spectrum and the acceptor's absorption spectrum overlap, and they are close together, FRET will occur. Efficient and fast FRET depends on the minimizing spatial separation between donor and acceptor. In the experiment, 4 and 5 MLs NPLs were mixed and act as donor and acceptor, respectively. A very fast FRET process was found with a time scale of 6 to 23 ps, which is smaller than the FRET time constant in QDs.[120] The large lateral size and the stacking contribute to the enhanced interaction between NPLs. Due to the fast FRET process in NPLs exceeds the rate of biexciton Auger recombination, the multiexciton energy transfer has been found in NPLs.[119] As mentioned earlier, the stacking of NPLs may also affect the PL properties at low temperatures. The reabsorption caused by stacking leads an amplification of phonon line.[63] Later, the dual emission of NPLs at low temperatures was thought to originate from excimer emission from stacking.[66] The stacking of NPLs has many effects on optical properties, so understanding and controlling is important in practical applications.

The unique 2D structure of NPLs not only makes it easy to form stacks, but also produces many special

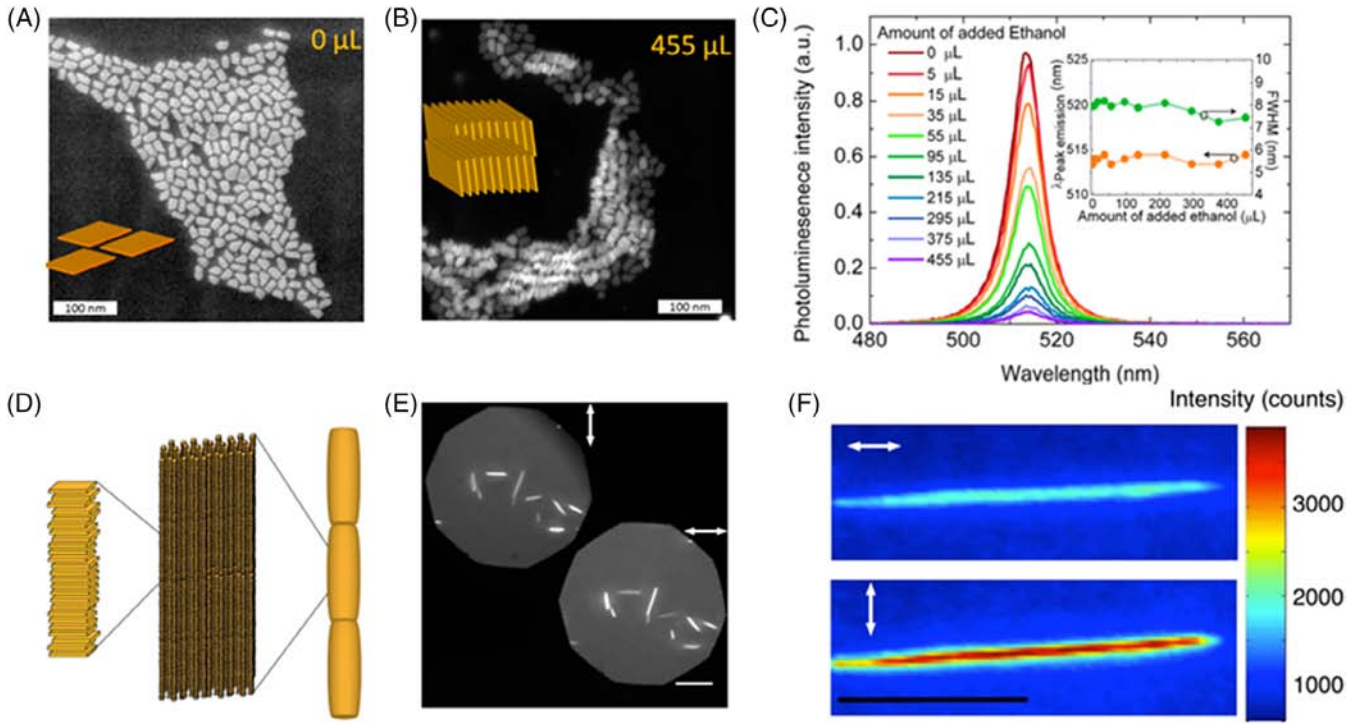

FIGURE 8 A,B, TEM images of CdSe NPLs with no ethanol and 455 μL ethanol. C, PL spectra of CdSe NPLs with adding different amount of ethanol. Inset shows the peak wavelength and FWHM as a function of amount of added ethanol. A,B,C, Copyright © 2014 American Chemical Society. D, Schematic diagram of the structure of superparticles stacked with CdSe NPLs. E, Fluorescence measurement of superparticles as a function of polarization direction. F, Fluorescence intensity of single superparticle depending on the polarization direction. D,E,F, Copyright © 2014 American Chemical Society. NPLs, nanoplatelets; PL, photoluminescence

changes in morphology. When the thickness is small while the lateral size is large, the NPLs easily form a scroll-like shape.[46,121-123] The reason for this structure formation is speculated to be the asymmetric constraints imposed by the carboxylic acid ligands on the NPLs surface.[121] In addition, nanohelix have been reported when the length of the lateral dimension is much greater than the width.[124] Stacking and twisting can even occur in the NPLs structure at the same time, and the parameters of this structure can also be adjusted by the lateral size of the NPLs.[125] At present, the PL properties of these special structure NPLs have not been found to be very different, but for other complex photophysical processes have not been studied, which may show some interesting properties.

3.5 | Metal halide perovskite nanoplatelets

As a new type of optoelectronic material, metal halide perovskite has received intensive attention in recent years. The general formula for metal halide perovskite structure is ABX_3, where A is monovalent cation, such as Cs^+, methylammonium (MA^+), or formamidinium (FA^+). B is a divalent cation (Pb^{2+}, Sn^{2+}), and X site is halide ion (Cl^{-1}, Br^{-1}, I^{-1}). Perovskite materials have shown great potential in photovoltaic applications, the efficiency of perovskite solar cells has exceeded 25% recently.[126] In addition, perovskite have also been applied in lasers,[127] photodetectors,[128] LEDs,[129] and other optoelectronic devices. Similar to CdSe materials, perovskite materials are also developing toward low-dimensional nanomaterials with various shape, such as QDs, nanorod, and NPLs.[130] For 2D metal halide perovskites, there are usually two structures, one of which is the two-dimensional Ruddlesden-Popper (2DRP) perovskite. The large aliphatic or alkylammonium cations, such as butylammonium (BA) and phenethylammonium (PEA), separates the 3D perovskite lattice into layers.[131,132] For this 2D layered perovskite, the thickness of each layers cannot be accurately controlled, so internal energy transfer processes usually occur in this material.[133,134] The other 2D perovskite is perovskite NPLs with thickness of only a few nanometers, similar to the CdSe NPLs. The earliest colloidal $MAPbBr_3$ perovskite NPLs were successfully synthesized in 2015.[135] Subsequently, the thickness of the colloidal perovskite NPLs was controlled by optimized synthesis method, and the $MAPbBr_3$ perovskite NPLs were successfully applied to LEDs.[136-138] However,

the inherent instability of organic cations prevents its further application. The appearance of all inorganic metal halide perovskite has greatly improved the stability of perovskite. Therefore, all-inorganic metal halide perovskite NPLs have also received great attention. The $CsPbBr_3$ NPLs was first reported in 2015, with thickness of only a few integer numbers of perovskite unit cells. In recent years, with the improvement of synthesis technology, there has been some progress in the control of its thickness and size.[139-146]

Compared with the 3D perovskite, the optical properties of the 2D colloidal perovskite NPLs have changed greatly, which are very similar to the CdSe NPLs. The absorption spectrum of perovskite NPLs produced a significant blue shift and dominated by an obvious exciton absorption peak.[139] The sharp exciton absorption peak indicates the strong electron-hole Coulomb interaction, which also proved that perovskite NPLs have large exciton binding energy. Some studies have shown that the exciton binding energy of perovskite NPL is in the range of 200 to 500 meV, which is much larger than the value of 3D perovskite.[147-149] The large exciton binding energy has greatly improved the radiation recombination efficiency of perovskite NPLs, which makes its PLQY value exceed 80%.[140] Similar to CdSe NPLs, the PL peak of the perovskite NPL exhibits a significant blue shift relative to the bulk material and showed a thickness-dependent change, which is an obvious feature of the quantum confinement effect in perovskite NPL. Different from CdSe NPLs, through the anion exchange method combined with the control of the thickness of NPLs, the all inorganic metal halide perovskite NPLs can achieve a wide range of emission tuning from ultraviolet to near infrared.[140,146,150] In addition, perovskite NPLs show stronger Auger recombination than CdSe NPLs, which is thought to be caused by the difference in band structure between these two materials.[151] The perovskite NPLs can self-assemble to form a stacked columnar structure, which is the same as the stacking characteristics of CdSe NPLs. In addition to this self-assembly method, it was found that the perovskite NPLs can also be fused with each other to form NPLs with larger lateral dimensions.[136,139] In recent years, inorganic metal halide perovskites have shown excellent optical gain performance.[152,153] However, unlike CdSe NPLs, colloidal inorganic metal halide perovskite NPLs have not been found to have strong optical gain, which remains to be further studied. At present, most of the researches mainly focus on the optimization of synthetic methods of colloidal inorganic metal halide perovskite NPLs, and the research on its optical properties is still lacking. In addition, the stability of perovskite NPLs is also a major problem in its application. There are many similarities between CdSe NPLs and perovskite NPLs, the research results of CdSe NPLs may contribute to the further development of perovskite NPLs.

4 | APPLICATIONS

4.1 | Nanoplatelets LED

In 1994, the emerge of the first colloidal QDs light-emitting diodes (LED) opened a new direction for LED technology.[154] Colloidal nanocrystals have the advantages of low cost, solution processability, and adjustable emission wavelength, which makes them promising luminescence materials. Most colloidal nanocrystals LEDs are currently based on spherical QDs.[155,156] Compared with QDs, NPLs have narrower emission peak, larger exciton binding energy, and faster radiation recombination rates, which make them more suitable as luminescent materials for LEDs. The narrow emission line of the NPLs is of great significance for the improvement of LED color purity, which is difficult to achieve by other materials.

The first NPLs-based LED was reported in 2013.[33] Figure 9A shows the structure of the LED device. CdSe/CdZnS core/shell NPLs were used as emissive material, which were deposited between organic and inorganic metal-oxide layers that serve as charge transport layers. The replacement of long-chain oleic acid ligands on the NPLs surface with short-chain 3-mer-captopropionic acid (MPA) or alkyldithiol has been shown to significantly improve charge injection and transport. Based on the optimized device structure, this NPLs LED exhibits a maximum luminance of 4499 cd/m^2 and an external quantum efficiency of 0.63%. It shows a narrow electroluminescence peak in 650 nm, and the range of FWHM is 25 to 30 nm, depending on the applied voltage. The narrowest electroluminescence (FWHM ~12.5 nm) colloidal nanocrystals LED was reported through CdSeS alloyed NPLs.[34] At the same time, the light emission wavelength of the LED can be adjusted by changing the ratio of Se and S. However, a very weak luminance (10-100 cd/m^2) was shown in this work, making it unusable in practice.

With the improvement of material synthesis technology and device structure, NPLs LEDs have shown greater application potential. A super color purity green NPLs LED was fabricated with CdSe/CdS NPLs, which exhibit a high external quantum efficiency of 5% and maximum luminance up to 33 000 cd/m^2 with a narrow electroluminescence spectra (~14 nm).[157] Through using a multifunctional polar and electrolytic polymer as electron transport layer material, a high efficiency NPL LED with saturated red electroluminescence was created.[158] This

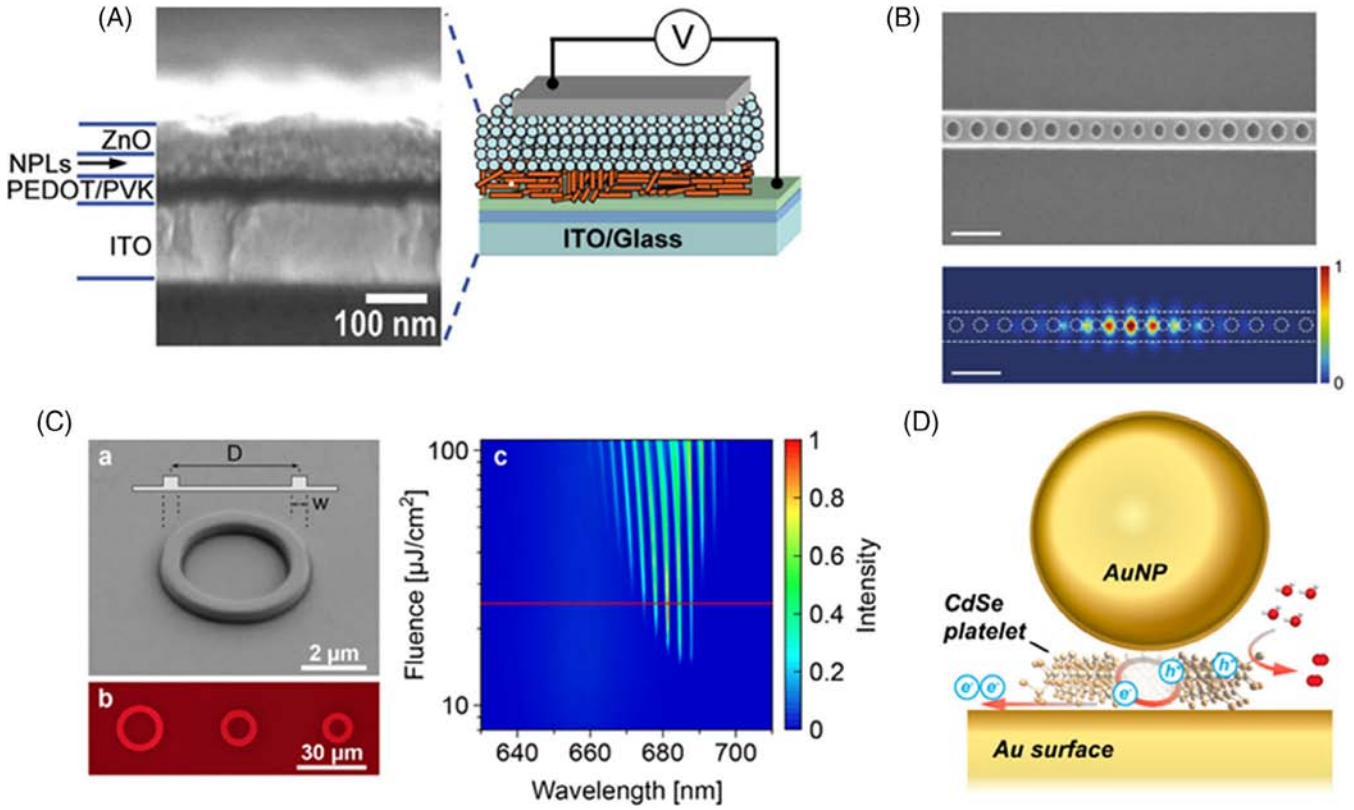

FIGURE 9 A, Cross-sectional SEM image and structure diagram of the NPLs LED device. Copyright © 2013 WILEY-VCH Verlag GmbH & Co. KGaA, Weinheim. B, SEM image of a Silicon nitride photonic-crystal nanobeam cavity and calculated electric-field intensity of the fundamental modal in this cavity. Copyright © 2017, Springer Nature. C, SEM image of a template-stripped NPLs ring resonator and the lasing of whispering gallery mode. Copyright © 2019 American Chemical Society. D, Schematic diagram of a photocatalytic water splitting device. The CdSe NPLs sandwich between Au nanoparticle and gold film. Copyright © 2015 American Chemical Society. LED, light-emitting diodes; NPLs, nanoplatelets

device achieves a high external quantum efficiency of 5.73%, which is an order of magnitude larger than the early red NPLs LED. Recently, the Cu-doped NPLs LEDs have been successfully realized.[159] When the doping concentration of Cu was 0.5%, dual emission was found in the LED. Moreover, it is interesting to find that the ratio of the two emission peaks can be changed by adjusting the device structure. Due to the special 2D shape of the NPLs, the arrangement during the deposition in the LED may affect the outcoupling efficiency, thereby improving the external quantum efficiency of the overall device. Controlling the NPLs film formation process may further improve the efficiency of the NPLs LED.[29,160]

4.2 | Lasers

Owing to excellent laser performance and low-cost processability, colloidal semiconductor nanocrystals are widely used in the research of laser. Various laser structures have been realized through combining QDs with simple optical cavities.[161-163] NPLs have been demonstrated to have large optical gains, therefore ASE can be achieved under very low excitation intensity. Integrating NPLs with optical cavities can obtain lower threshold lasers.

In 2004, Guzelturk et al used the all solution-processed distributed Bragg reflectors (DBR), which made by staggered stacking of SiO_2 and TiO_2 nanoparticles, to serve as optical cavity.[35] CdSe/CdS core/crown NPLs were deposited between two DBRs to form vertical cavity surface-emitting laser (VCSEL) structure. In the case of two-photon pumping, a laser threshold of 2.49 mJ/cm^2 was obtained. In the same year, Grim et al also used two DBRs as optical cavities, and used CdSe NPLs as optical gain materials to achieve continuous-wave pumped laser emission at a power density of 440 W/cm^2.[55] However, with the continuous pumping under high-power density, the output intensity of the lasers will decrease significantly. In 2005, Li et al used the CdSe NPLs solution as a gain material, and directly used a cuvette as an optical resonant cavity,

single-photon, two-photon, and three-photon laser emission was successfully achieved in solution.[114] Laser performance can be improved by increasing the optical gain properties of the NPLs material, while another approach is to design an optical cavity with a higher quality factor. The lasing with an ultra-low threshold of 0.97 μW was demonstrated through the combination of CdSe/CdS core/shell NPLs with silicon-nitride nanobeam cavities as shown in Figure 9B.[98] This laser supports room temperature continuous-wave operation, which can be attributed to the high optical gain of NPLs, along with the high quality factor of nanocavities. Recently, the use of a ring resonator and NPLs to achieve laser emission in the whispering gallery mode has also been realized.[37] Figure 9C shows the structure of micro ring resonator and the lasing in whispering gallery mode.

4.3 | Other

In addition to the two applications above, the unique shape and properties of the NPLs also brings more possibilities in application. Luminescent solar concentrator (LSC) is a type of light-harvesting device. The luminescent material sandwiched between two transparent plastic plates absorbs sunlight and emits longer-wavelength light, which reaches the edge of the plastic plate through total reflection, and is finally converted into electricity by solar cells. The Cu-doped CdSe NPLs was found to be very suitable for apply in the LSC due to the high PL QY, large Stokes shift and high absorption cross section.[50] NPLs have also proven to be an excellent photocatalytic platform. In 2005, Naskar et al reported a synthetic method that enables site-selective growth of noble metal on NPLs.[164] By changing the growth parameters, Au, Pt, Pd can be grown on CdSe NPLs, which creates a good platform for the realization of photocatalysis. As the noble metal grows, the emission of the NPLs is gradually quenched. The results of femtosecond TA prove that electrons are transferred from the NPLs to the noble metal in a very short time (~800 fs).[165] The photocatalytic decomposition of methylene blue and methyl orange in aqueous solution was realized using CdSe/CdS-Au hybrid NPLs.[165] In addition, the ultra-thin nature of NPLs is also used for photocatalysis, the device structure is shown in Figure 9D. The NPLs was placed in the nanogap formed by the Au nanoparticle and the gold film, and enhanced plasmonic fields increased the efficiency of photocatalytic water splitting.[38] The large surface area of NPLs makes them a promising platform for sensing. It was found that the increase of oxygen concentration can improve the PL efficiency of NPLs, this is mainly due to the hole trapping by surface defects. Therefore, CdSe NPLs can be used to realize oxygen sensing.[39] Moreover, CdSeS NPLs have been used for organophosphorus pesticide detection.[166]

5 | SUMMARY AND PROSPECTS

In summary, this article reviews the emergence and development of 2D CdSe NPLs in recent years. Compared with QDs and nanorod, as the latest structure in the colloidal semiconductor nanocrystal system, the 2D NPLs exhibit many special properties. CdSe NPLs usually have only 3 to 5 MLs in thickness, which is smaller than the exciton Bohr radius, while their lateral dimensions are large. Therefore, quantum confinement exists only in the thickness direction, which determines the optical properties of the CdSe NPLs. The atomic precision of thickness eliminates inhomogeneous broadening, which enables very narrow emission line. In addition, the strong 1D confinement and large surface area induce a large exciton binding energy, fast radiation recombination rate, and large absorption cross-sections. Core-shell and core-crown heterostructures introduce more possibilities for the control of optical properties of CdSe NPLs. By changing the material of the shell or crown, it is possible to realize broadband emission of CdSe NPLs from visible to near-infrared. At the same time, the PLQY and stability of the CdSe NPLs have also been improved. CdSe NPLs exhibit higher optical gain than other colloidal semiconductor nanocrystals, which results in an ultra-low ASE threshold. Band engineering or gradient alloy structure of the shell or crown can further optimize the optical gain performance of the CdSe NPLs. These excellent properties of CdSe NPLs have been successfully applied in to LEDs and Lasers, realizing super color purity LED and ultra-low threshold nanolaser. In addition, CdSe NPLs also show potential in the application of LSC, photocatalysis, and sensing.

Although CdSe NPLs have many impressive optical properties, there are still some problems and challenges. First, for the application of optoelectronic devices, colloidal NPLs usually exist in the form of deposited films. However, due to the plane shape of the NPLs, they are easily self-stacking, which has been shown to affect their optical properties. Such stacking may reduce device performance, so further research may be needed to better control the alignment state of the NPLs deposition. Second, although NPLs-based LEDs have been realized with a narrow emission, the efficiency is still very low. There have been many studies on the optimization of the optical properties of NPLs, but the device structure of LEDs is still lagging. Therefore, the optimization of the device structure is critical for the practical application of NPLs LEDs. Third, the mechanism of optical gain in NPLs

needs to be further studied, such as how the lateral size and thickness affect its gain performance. In this way, lower threshold NPLs lasers can be achieved by optimizing the structural parameters. In addition, although continuous wave pumped laser at room temperature by the NPLs have been achieved, how to realize electric drive laser by NPLs is still a big challenge.

ACKNOWLEDGMENTS

This work is supported by the National Natural Science Foundation of China (11574130), Shenzhen Science and Technology Innovation Commission (Projects nos. KQJSCX20170726145748464, JCYJ20180305180553701, and KQTD2015071710313656).

CONFLICT OF INTEREST

The authors declare no potential conflict of interest.

ORCID

Rui Chen https://orcid.org/0000-0002-0445-7847

REFERENCES

1. Ekimov AI, Onushchenko AA. Quantum size effect in 3-dimensional microscopic semiconductor crystals. *JETP Lett*. 1981;34:345-349.
2. Ekimov AI, Efros AL. Nonlinear optics of semiconductor-doped glasses. *Phys Status Solidi B*. 1988;150:627-633.
3. Grabovskis VJ, Dzenis JJ, Ekimov AI, Kudryavtsev IA, Tolstoi MN, Rogulis UT. Photoionization of semiconductor microcrystals in glass. *Fiz Tverd Tela*. 1989;311:272-275.
4. Murray CB, Norris DJ, Bawendi MG. Synthesis and characterization of nearly monodisperse CdE (E = S, Se, Te) semiconductor nanocrystallites. *J Am Chem Soc*. 1993;115:8706-8715.
5. Smith AM, Nie SM. Semiconductor nanocrystals: structure, properties, and band gap engineering. *Acc Chem Res*. 2010;43:190-200.
6. Reiss P, Protiere M, Li L. Core/Shell semiconductor nanocrystals. *Small*. 2009;5:154-168.
7. Vasudevan D, Gaddam RR, Trinchi A, Cole I. Core-shell quantum dots: properties and applications. *J Alloy Compd*. 2015;636:395-404.
8. Vaxenburg R, Rodina A, Lifshitz E, Le A. Biexciton auger recombination in CdSe/CdS core/shell semiconductor nanocrystals. *Nano Lett*. 2016;16:2503-2511.
9. Oron D, Kazes M, Banin U. Multiexcitons in type-II colloidal semiconductor quantum dots. *Phys Rev B*. 2007;75:035330.
10. Wang Y, Ta VD, Gao Y, et al. Stimulated emission and lasing from CdSe/CdS/ZnS core-multi-shell quantum dots by simultaneous three-photon absorption. *Adv Mater*. 2014;26:2954-2961.
11. Mashford BS, Stevenson M, Popovic Z, et al. High-efficiency quantum-dot light-emitting devices with enhanced charge injection. *Nat Photonics*. 2013;7:407-412.
12. Dai X, Deng Y, Peng X, Jin Y. Quantum-dot light-emitting diodes for large-area displays: towards the dawn of commercialization. *Adv Mater*. 2017;29:1607022.
13. Supran GJ, Shirasaki Y, Song KW, et al. QLEDs for displays and solid-state lighting. *MRS Bull*. 2013;38:703-711.
14. Michalet X, Pinaud FF, Bentolila LA, et al. Quantum dots for live cells, in vivo imaging, and diagnostics. *Science*. 2005;307:538-544.
15. Medintz IL, Uyeda HT, Goldman ER, Mattoussi H. Quantum dot bioconjugates for imaging, labelling and sensing. *Nat Mater*. 2005;4:435-446.
16. Klimov VI, Mikhailovsky AA, Xu S, et al. Optical gain and stimulated emission in nanocrystal quantum dots. *Science*. 2000;290:314-317.
17. Wang Y, Li X, Song J, Xiao L, Zeng H, Sun H. All-inorganic colloidal perovskite quantum dots: a new class of lasing materials with favorable characteristics. *Adv Mater*. 2015;27:7101-7108.
18. Dang C, Lee J, Breen C, Steckel JS, Coe-Sullivan S, Nurmikko A. Red, green and blue lasing enabled by single-exciton gain in colloidal quantum dot films. *Nat Nanotechnol*. 2012;7:335-339.
19. Peng XG, Manna L, Yang WD, et al. Shape control of CdSe nanocrystals. *Nature*. 2000;404:59-61.
20. Sitt A, Hadar I, Banin U. Band-gap engineering, optoelectronic properties and applications of colloidal heterostructured semiconductor nanorods. *Nano Today*. 2013;8:494-513.
21. Joo J, Son JS, Kwon SG, Yu JH, Hyeon T. Low-temperature solution-phase synthesis of quantum well structured CdSe nanoribbons. *J Am Chem Soc*. 2006;128:5632-5633.
22. Ithurria S, Tessier MD, Mahler B, Lobo RP, Dubertret B, Efros AL. Colloidal nanoplatelets with two-dimensional electronic structure. *Nat Mater*. 2011;10:936-941.
23. Bouet C, Tessier MD, Ithurria S, Mahler B, Nadal B, Dubertret B. Flat colloidal semiconductor nanoplatelets. *Chem Mater*. 2013;25:1262-1271.
24. Pelton M. Carrier dynamics, optical gain, and lasing with colloidal quantum wells. *J Phys Chem C*. 2018;122:10659-10674.
25. Ithurria S, Talapin DV. Colloidal atomic layer deposition (c-ALD) using self-limiting reactions at nanocrystal surface coupled to phase transfer between polar and nonpolar media. *J Am Chem Soc*. 2012;134:18585-18590.
26. Rossinelli AA, Riedinger A, Marques-Gallego P, Knusel PN, Antolinez FV, Norris DJ. High-temperature growth of thick-shell CdSe/CdS core/shell nanoplatelets. *Chem Commun*. 2017;53:9938-9941.
27. Prudnikau A, Chuvilin A, Artemyev M. CdSe-CdS nanoheteroplatelets with efficient photoexcitation of central CdSe region through epitaxially grown CdS wings. *J Am Chem Soc*. 2013;135:14476-14479.
28. Tessier MD, Spinicelli P, Dupont D, Patriarche G, Ithurria S, Dubertret B. Efficient exciton concentrators built from colloidal core/crown CdSe/CdS semiconductor nanoplatelets. *Nano Lett*. 2014;14:207-213.
29. Shendre S, Delikanli S, Li M, et al. Ultrahigh-efficiency aqueous flat nanocrystals of CdSe/CdS@$Cd_{1-x}Zn_xS$ colloidal core/crown@alloyed-shell quantum wells. *Nanoscale*. 2018;11:301-310.
30. Dede D, Taghipour N, Quliyeva U, et al. Highly stable multicrown heterostructures of type-ii nanoplatelets for ultralow threshold optical gain. *Chem Mater*. 2019;31:1818-1826.

31. Guzelturk B, Erdem O, Olutas M, Kelestemur Y, Demir HV. Stacking in colloidal nanoplatelets: tuning excitonic properties. *ACS Nano*. 2014;8:12524-12533.
32. Erdem O, Olutas M, Guzelturk B, Kelestemur Y, Demir HV. Temperature-dependent emission kinetics of colloidal semiconductor nanoplatelets strongly modified by stacking. *J Phys Chem Lett*. 2016;7:548-554.
33. Chen ZY, Nadal B, Mahler B, Aubin H, Dubertret B. Quasi-2D colloidal semiconductor nanoplatelets for narrow electroluminescence. *Adv Funct Mater*. 2014;24:295-302.
34. Fan F, Kanjanaboos P, Saravanapavanantham M, et al. Colloidal $CdSe_{1-x}S_x$ nanoplatelets with narrow and continuously-tunable electroluminescence. *Nano Lett*. 2015;15:4611-4615.
35. Guzelturk B, Kelestemur Y, Olutas M, Delikanli S, Demir HV. Amplified spontaneous emission and lasing in colloidal nanoplatelets. *ACS Nano*. 2014;8:6599-6605.
36. Altintas Y, Gungor K, Gao Y, et al. Giant alloyed hot injection shells enable ultralow optical gain threshold in colloidal quantum wells. *ACS Nano*. 2019;13:10662-10670.
37. Rossinelli AA, Rojo H, Mule AS, et al. Compositional grading for efficient and narrowband emission in CdSe-based core/shell nanoplatelets. *Chem Mater*. 2019;31:9567-9578.
38. Sigle DO, Zhang L, Ithurria S, Dubertret B, Baumberg JJ. Ultrathin CdSe in plasmonic nanogaps for enhanced photocatalytic water splitting. *J Phys Chem Lett*. 2015;6:1099-1103.
39. Lorenzon M, Christodoulou S, Vaccaro G, et al. Reversed oxygen sensing using colloidal quantum wells towards highly emissive photoresponsive varnishes. *Nat Commun*. 2015;6:6434.
40. Ithurria S, Dubertret B. Quasi 2d colloidal CdSe platelets with thicknesses controlled at the atomic level. *J Am Chem Soc*. 2008;130:16504-16505.
41. Ithurria S, Bousquet G, Dubertret B. Continuous transition from 3D to 1D confinement observed during the formation of CdSe nanoplatelets. *J Am Chem Soc*. 2011;133:3070-3077.
42. Chen YY, Chen DD, Li Z, Peng XG. Symmetry-breaking for formation of rectangular cdse two-dimensional nanocrystals in zinc-blende structure. *J Am Chem Soc*. 2017;139:10009-10019.
43. Delikanli S, Yu G, Yeltik A, et al. Ultrathin highly luminescent two-monolayer colloidal CdSe nanoplatelets. *Adv Funct Mater*. 2019;29:1901028.
44. Chu A, Livache C, Ithurria S, Lhuillier E. Electronic structure robustness and design rules for 2D colloidal heterostructures. *J Appl Phys*. 2018;123:035701.
45. Christodoulou S, Climente JI, Planelles J, et al. Chloride-induced thickness control in CdSe nanoplatelets. *Nano Lett*. 2018;18:6248-6254.
46. Mahler B, Nadal B, Bouet C, Patriarche G, Dubertret B. Core/shell colloidal semiconductor nanoplatelets. *J Am Chem Soc*. 2012;134:18591-18598.
47. Altintas Y, Quliyeva U, Gungor K, et al. Highly stable, near-unity efficiency atomically flat semiconductor nanocrystals of CdSe/ZnS hetero-nanoplatelets enabled by ZnS-shell hot-injection growth. *Small*. 2019;15:1804854.
48. Pedetti S, Ithurria S, Heuclin H, Patriarche G, Dubertret B. Type-II CdSe/CdTe core/crown semiconductor nanoplatelets. *J Am Chem Soc*. 2014;136:16430-16438.
49. Delikanli S, Guzelturk B, Hernandez-Martinez PL, et al. Continuously tunable emission in inverted type-I CdS/CdSe Core/crown semiconductor nanoplatelets. *Adv Funct Mater*. 2015;25:4282-4289.
50. Sharma M, Gungor K, Yeltik A, et al. Near-unity emitting copper-doped colloidal semiconductor quantum wells for luminescent solar concentrators. *Adv Mater*. 2017;29:1700821.
51. Galle T, Kazes M, Hübner R, et al. Colloidal mercury-doped CdSe nanoplatelets with dual fluorescence. *Chem Mater*. 2019;31:5065-5074.
52. Sharma M, Olutas M, Yeltik A, et al. Understanding the journey of dopant copper ions in atomically flat colloidal nanocrystals of CdSe nanoplatelets using partial cation exchange reactions. *Chem Mater*. 2018;30:3265-3275.
53. Achtstein AW, Schliwa A, Prudnikau A, et al. Electronic structure and exciton-phonon interaction in two-dimensional colloidal CdSe nanosheets. *Nano Lett*. 2012;12:3151-3157.
54. Naeem A, Masia F, Christodoulou S, Moreels I, Borri P, Langbein W. Giant exciton oscillator strength and radiatively limited dephasing in two-dimensional platelets. *Phys Rev B*. 2015;91:121302.
55. Grim JQ, Christodoulou S, Di Stasio F, et al. Continuous-wave biexciton lasing at room temperature using solution-processed quantum wells. *Nat Nanotechnol*. 2014;9:891-895.
56. Achtstein AW, Marquardt O, Scott R, et al. Impact of shell growth on recombination dynamics and exciton-phonon interaction in CdSe-CdS core-shell nanoplatelets. *ACS Nano*. 2018;12:9476-9483.
57. Zelewski SJ, Nawrot KC, Zak A, Gladysiewicz M, Nyk M, Kudrawiec R. Exciton binding energy of two-dimensional highly luminescent colloidal nanostructures determined from combined optical and photoacoustic spectroscopies. *J Phys Chem Lett*. 2019;10:3459-3464.
58. Tessier MD, Javaux C, Maksimovic I, Loriette V, Dubertret B. Spectroscopy of single CdSe nanoplatelets. *ACS Nano*. 2012;6:6751-6758.
59. Leatherdale CA, Woo WK, Mikulec FV, Bawendi MG. On the absorption cross section of CdSe nanocrystal quantum dots. *J Phys Chem B*. 2002;106:7619-7622.
60. She C, Fedin I, Dolzhnikov DS, et al. Low-threshold stimulated emission using colloidal quantum wells. *Nano Lett*. 2014;14:2772-2777.
61. Yeltik A, Delikanli S, Olutas M, Kelestemur Y, Guzelturk B, Demir HV. Experimental determination of the absorption cross-section and molar extinction coefficient of colloidal CdSe nanoplatelets. *J Phys Chem C*. 2015;119:26768-26775.
62. Achtstein AW, Antanovich A, Prudnikau A, Scott R, Woggon U, Artemyev M. Linear absorption in CdSe nanoplates: thickness and lateral size dependency of the intrinsic absorption. *J Phys Chem C*. 2015;119:20156-20161.
63. Tessier MD, Biadala L, Bouet C, Ithurria S, Abecassis B, Dubertret B. Phonon line emission revealed by self-assembly of colloidal nanoplatelets. *ACS Nano*. 2013;7:3332-3340.
64. Achtstein AW, Scott R, Kickhofel S, et al. p-State luminescence in CdSe nanoplatelets: role of lateral confinement and a longitudinal optical phonon bottleneck. *Phys Rev Lett*. 2016;116:116802.

65. Shornikova EV, Biadala L, Yakovlev DR, et al. Addressing the exciton fine structure in colloidal nanocrystals: the case of CdSe nanoplatelets. *Nanoscale*. 2018;10:646-656.
66. Diroll BT, Cho W, Coropceanu I, et al. Semiconductor nanoplatelet excimers. *Nano Lett*. 2018;18:6948-6953.
67. Yu J, Zhang C, Pang G, Sun XW, Chen R. Effect of lateral size and surface passivation on the near-band-edge excitonic emission from quasi-two-dimensional CdSe nanoplatelets. *ACS Appl Mater Interfaces*. 2019;11:41821-41827.
68. Cho W, Kim S, Coropceanu I, et al. Direct synthesis of six-monolayer (1.9 nm) thick zinc-blende CdSe nanoplatelets emitting at 585 nm. *Chem Mater*. 2018;30:6957-6960.
69. Tessier MD, Mahler B, Nadal B, Heuclin H, Pedetti S, Dubertret B. Spectroscopy of colloidal semiconductor core/shell nanoplatelets with high quantum yield. *Nano Lett*. 2013;13:3321-3328.
70. Polovitsyn A, Dang Z, Movilla JL, et al. Synthesis of air-stable CdSe/ZnS core–shell nanoplatelets with tunable emission wavelength. *Chem Mater*. 2017;29:5671-5680.
71. Li Q, Wu K, Chen J, Chen Z, Mcbride JR, Lian T. Size-independent exciton localization efficiency in colloidal CdSe/CdS core/crown nanosheet type-I heterostructures. *ACS Nano*. 2016;10:3843-3851.
72. Antanovich AV, Prudnikau AV, Melnikau D, et al. Colloidal synthesis and optical properties of type-II CdSe-CdTe and inverted CdTe-CdSe core-wing heteronanoplatelets. *Nanoscale*. 2015;7:8084-8092.
73. Kelestemur Y, Olutas M, Delikanli S, Guzelturk B, Akgul MZ, Demir HV. Type-II colloidal quantum wells: CdSe/CdTe core/crown heteronanoplatelets. *J Phys Chem C*. 2015;119:2177-2185.
74. Dufour M, Steinmetz V, Izquierdo E, et al. Engineering bicolor emission in 2D core/crown $CdSe/CdSe_{1-x}Te_x$ nanoplatelet heterostructures using band-offset tuning. *J Phys Chem C*. 2017;121:24816-24823.
75. Kelestemur Y, Guzelturk B, Erdem O, et al. $CdSe/CdSe_{1-x}Te_x$ core/crown heteronanoplatelets: tuning the excitonic properties without changing the thickness. *J Phys Chem C*. 2017;121:4650-4658.
76. Liu B, Delikanli S, Gao Y, Dede D, Gungor K, Demir HV. Nanocrystal light-emitting diodes based on type II nanoplatelets. *Nano Energy*. 2018;47:115-122.
77. Yu JH, Liu X, Kweon KE, et al. Giant Zeeman splitting in nucleation-controlled doped $CdSe:Mn^{2+}$ quantum nanoribbons. *Nat Mater*. 2010;9:47-53.
78. Sharma A, Sharma M, Gungor K, Olutas M, Dede D, Demir HV. Near-infrared-emitting five-monolayer thick copper-doped CdSe nanoplatelets. *Adv Opt Mater*. 2019;7:1900831.
79. Khan AH, Pinchetti V, Tanghe I, et al. Tunable and efficient red to near-infrared photoluminescence by synergistic exploitation of core and surface silver doping of CdSe nanoplatelets. *Chem Mater*. 2019;31:1450-1459.
80. Dufour M, Izquierdo E, Livache C, et al. Doping as a strategy to tune color of 2D colloidal nanoplatelets. *ACS Appl Mater Interfaces*. 2019;11:10128-10134.
81. Schlenskaya NN, Yao Y, Mano T, et al. Scroll-like alloyed CdS_xSe_{1-x} nanoplatelets: facile synthesis and detailed analysis of tunable optical properties. *Chem Mater*. 2017;29:579-586.
82. Antanovich A, Achtstein AW, Matsukovich A, et al. A strain-induced exciton transition energy shift in CdSe nanoplatelets: the impact of an organic ligand shell. *Nanoscale*. 2017;9:18042-18053.
83. Dufour M, Qu J, Greboval C, Methivier C, Lhuillier E, Ithurria S. Halide ligands to release strain in cadmium chalcogenide nanoplatelets and achieve high brightness. *ACS Nano*. 2019;13:5326-5334.
84. Pelton M, Ithurria S, Schaller RD, Dolzhnikov DS, Talapin DV. Carrier cooling in colloidal quantum wells. *Nano Lett*. 2012;12:6158-6163.
85. Baghani E, O'leary SK, Fedin I, Talapin DV, Pelton M. Auger-limited carrier recombination and relaxation in CdSe colloidal quantum wells. *J Phys Chem Lett*. 2015;6:1032-1036.
86. Sippel P, Albrecht W, Van Der Bok JC, et al. Femtosecond cooling of hot electrons in CdSe quantum-well platelets. *Nano Lett*. 2015;15:2409-2416.
87. Nozik AJ. Spectroscopy and hot electron relaxation dynamics in semiconductor quantum wells and quantum dots. *Annu Rev Phys Chem*. 2001;52:193-231.
88. Kunneman LT, Schins JM, Pedetti S, et al. Nature and decay pathways of photoexcited states in CdSe and CdSe/CdS nanoplatelets. *Nano Lett*. 2014;14:7039-7045.
89. Rabouw FT, Van Der Bok JC, Spinicelli P, et al. Temporary charge carrier separation dominates the photoluminescence decay dynamics of colloidal CdSe nanoplatelets. *Nano Lett*. 2016;16:2047-2053.
90. Rabouw FT, Kamp M, Van Dijk-Moes RJ, et al. Delayed exciton emission and its relation to blinking in CdSe quantum dots. *Nano Lett*. 2015;15:7718-7725.
91. Wu K, Li Q, Du Y, Chen Z, Lian T. Ultrafast exciton quenching by energy and electron transfer in colloidal CdSe nanosheet-Pt heterostructures. *Chem Sci*. 2015;6:1049-1054.
92. Li Q, Zhou B, Mcbride JR, Lian T. Efficient diffusive transport of hot and cold excitons in colloidal type ii CdSe/CdTe core/crown nanoplatelet heterostructures. *ACS Energy Lett*. 2016;2:174-181.
93. Wu KF, Li QY, Jia YY, Mcbride JR, Xie ZX, Lian TQ. Efficient and ultrafast formation of long-lived charge-transfer exciton state in atomically thin cadmium selenide/cadmium telluride type-II heteronanosheets. *ACS Nano*. 2015;9:961-968.
94. Yadav S, Singh A, Sapra S. Long-lived emission in type-II CdS/ZnSe core/crown nanoplatelet heterostructures. *J Phys Chem C*. 2017;121:27241-27246.
95. Pandya R, Chen RYS, Cheminal A, et al. Exciton-phonon interactions govern charge-transfer-state dynamics in CdSe/CdTe two-dimensional colloidal heterostructures. *J Am Chem Soc*. 2018;140:14097-14111.
96. Li Q, Lian T. Area- and thickness-dependent biexciton auger recombination in colloidal CdSe nanoplatelets: breaking the "universal volume scaling law". *Nano Lett*. 2017;17:3152-3158.
97. Kunneman LT, Tessier MD, Heuclin H, et al. Bimolecular auger recombination of electron–hole pairs in two-dimensional CdSe and CdSe/CdZnS core/shell nanoplatelets. *J Phys Chem Lett*. 2013;4:3574-3578.
98. Yang Z, Pelton M, Fedin I, Talapin DV, Waks E. A room temperature continuous-wave nanolaser using colloidal quantum wells. *Nat Commun*. 2017;8:143.

99. Li Q, Lian T. A model for optical gain in colloidal nanoplatelets. *Chem Sci*. 2018;9:728-734.
100. Klimov VI. Quantization of multiparticle Auger rates in semiconductor quantum dots. *Science*. 2000;287:1011-1013.
101. Malko AV, Mikhailovsky AA, Petruska MA, Hollingsworth JA, Klimov VI. Interplay between optical gain and photoinduced absorption in CdSe nanocrystals. *J Phys Chem B*. 2004;108:5250-5255.
102. Ma X, Diroll BT, Cho W, et al. Size-dependent biexciton quantum yields and carrier dynamics of quasi-two-dimensional core/shell nanoplatelets. *ACS Nano*. 2017;11:9119-9127.
103. She CX, Fedin I, Dolzhnikov DS, et al. Red, yellow, green, and blue amplified spontaneous emission and lasing using colloidal CdSe nanoplatelets. *ACS Nano*. 2015;9:9475-9485.
104. Malko AV, Mikhailovsky AA, Petruska MA, et al. From amplified spontaneous emission to microring lasing using nanocrystal quantum dot solids. *Appl Phys Lett*. 2002;81:1303-1305.
105. Htoon H, Hollingworth JA, Malko AV, Dickerson R, Klimov VI. Light amplification in semiconductor nanocrystals: quantum rods versus quantum dots. *Appl Phys Lett*. 2003;82:4776-4778.
106. Shaklee KL, Leheny RF. Direct determination of optical gain in semiconductor crystals. *Appl Phys Lett*. 1971;18:475-477.
107. Guzelturk B, Kelestemur Y, Olutas M, Li Q, Lian T, Demir HV. High-efficiency optical gain in type-II semiconductor nanocrystals of alloyed colloidal quantum wells. *J Phys Chem Lett*. 2017;8:5317-5324.
108. Guzelturk B, Pelton M, Olutas M, Demir HV. Giant modal gain coefficients in colloidal II-VI nanoplatelets. *Nano Lett*. 2019;19:277-282.
109. Olutas M, Guzelturk B, Kelestemur Y, Yeltik A, Delikanli S, Demir HV. Lateral size-dependent spontaneous and stimulated emission properties in colloidal CdSe nanoplatelets. *ACS Nano*. 2015;9:5041-5050.
110. Li Q, Xu Z, Mcbride JR, Lian T. Low threshold multiexciton optical gain in colloidal CdSe/CdTe core/crown type-II nanoplatelet heterostructures. *ACS Nano*. 2017;11:2545-2553.
111. Gao Y, Li M, Delikanli S, et al. Low-threshold lasing from colloidal CdSe/CdSeTe core/alloyed-crown type-II heteronanoplatelets. *Nanoscale*. 2018;10:9466-9475.
112. Chou K-L, Won N, Kwag J, Kim S, Chen J-Y. Femto-second laser beam with a low power density achieved a two-photon photodynamic cancer therapy with quantum dots. *J Mater Chem B*. 2013;1:4584.
113. He T, Qiu X, Li J, et al. Water-soluble chiral CdSe/CdS dot/-rod nanocrystals for two-photon fluorescence lifetime imaging and photodynamic therapy. *Nanoscale*. 2019;11:15245-15252.
114. Li M, Zhi M, Zhu H, et al. Ultralow-threshold multiphoton-pumped lasing from colloidal nanoplatelets in solution. *Nat Commun*. 2015;6:8513.
115. Guzelturk B, Kelestemur Y, Gungor K, et al. Stable and low-threshold optical gain in CdSe/CdS quantum dots: an all-colloidal frequency up-converted laser. *Adv Mater*. 2015;27:2741-2746.
116. Scott R, Achtstein AW, Prudnikau A, et al. Two photon absorption in II-VI semiconductors: the influence of dimensionality and size. *Nano Lett*. 2015;15:4985-4992.
117. Crooker SA, Hollingsworth JA, Tretiak S, Klimov VI. Spectrally resolved dynamics of energy transfer in quantum-dot assemblies: towards engineered energy flows in artificial materials. *Phys Rev Lett*. 2002;89:186802.
118. Abecassis B, Tessier MD, Davidson P, Dubertret B. Self-assembly of CdSe nanoplatelets into giant micrometer-scale needles emitting polarized light. *Nano Lett*. 2014;14:710-715.
119. Miethe JF, Schlosser A, Eckert JG, Lübkemann F, Bigall NC. Electronic transport in CdSe nanoplatelet based polymer fibres. *J Mater Chem C*. 2018;6:10916-10923.
120. Rowland CE, Fedin I, Zhang H, et al. Picosecond energy transfer and multiexciton transfer outpaces auger recombination in binary CdSe nanoplatelet solids. *Nat Mater*. 2015;14:484-489.
121. Achermann M, Petruska MA, Crooker SA, Klimov VI. Picosecond energy transfer in quantum dot Langmuir-Blodgett nanoassemblies. *J Phys Chem B*. 2003;107:13782-13787.
122. Bouet C, Mahler B, Nadal B, et al. Two-dimensional growth of CdSe nanocrystals, from nanoplatelets to nanosheets. *Chem Mater*. 2013;25:639-645.
123. Kurtina DA, Garshev AV, Vasil'eva IS, Shubin VV, Gaskov AM, Vasiliev RB. Atomically thin population of colloidal CdSe nanoplatelets: growth of rolled-up nanosheets and strong circular dichroism induced by ligand exchange. *Chem Mater*. 2019;31:9652-9663.
124. Liu Y, Rowell N, Willis M, et al. Photoluminescent colloidal nanohelices self-assembled from CdSe magic-size clusters via nanoplatelets. *J Phys Chem Lett*. 2019;10:2794-2801.
125. Kim WD, Yoon D-E, Kim D, et al. Stacking of colloidal CdSe nanoplatelets into twisted ribbon superstructures: origin of twisting and its implication in optical properties. *J Phys Chem C*. 2019;12314:9445-9453.
126. Luo D, Su R, Zhang W, Gong Q, Zhu R. Minimizing non-radiative recombination losses in perovskite solar cells. *Nat Rev Mater*. 2019;5:44-60.
127. Wei Q, Li X, Liang C, et al. Recent Progress in metal halide perovskite micro- and nanolasers. *Adv Opt Mater*. 2019;7:1900080.
128. Tian W, Zhou H, Li L. Hybrid organic-inorganic perovskite photodetectors. *Small*. 2017;13:1702107.
129. Veldhuis SA, Boix PP, Yantara N, et al. Perovskite materials for light-emitting diodes and lasers. *Adv Mater*. 2016;28:6804-6834.
130. Aamir M, Adhikari T, Sher M, Khan MD, Akhtar J, Nunzi JM. Cesium lead halide perovskite nanostructures: tunable morphology and halide composition. *Chem Rec*. 2018;18:230-238.
131. Zheng Y, Niu T, Ran X, et al. Unique characteristics of 2D Ruddlesden-Popper (2DRP) perovskite for future photovoltaic application. *J Mat Chem A*. 2019;7:13860-13872.
132. Zhou C, Lin H, He Q, et al. Low dimensional metal halide perovskites and hybrids. *Mater Sci Eng R Rep*. 2019;137:38-65.
133. Proppe AH, Quintero-Bermudez R, Tan H, Voznyy O, Kelley SO, Sargent EH. Synthetic control over quantum well width distribution and carrier migration in low-dimensional perovskite photovoltaics. *J Am Chem Soc*. 2018;140:2890-2896.

134. Shang Q, Wang Y, Zhong Y, et al. Unveiling structurally engineered carrier dynamics in hybrid quasi-two-dimensional perovskite thin films toward controllable emission. *J Phys Chem Lett*. 2017;8:4431-4438.
135. Tyagi P, Arveson SM, Tisdale WA. Colloidal organohalide perovskite nanoplatelets exhibiting quantum confinement. *J Phys Chem Lett*. 2015;6:1911-1916.
136. Sichert JA, Tong Y, Mutz N, et al. Quantum size effect in organometal halide perovskite nanoplatelets. *Nano Lett*. 2015; 15:6521-6527.
137. Kumar S, Jagielski J, Yakunin S, et al. Efficient blue electroluminescence using quantum-confined two-dimensional perovskites. *ACS Nano*. 2016;10:9720-9729.
138. Ling Y, Yuan Z, Tian Y, et al. Bright light-emitting diodes based on organometal halide perovskite nanoplatelets. *Adv Mater*. 2016;28:305-311.
139. Bekenstein Y, Koscher BA, Eaton SW, Yang P, Alivisatos AP. Highly luminescent colloidal nanoplates of perovskite cesium lead halide and their oriented assemblies. *J Am Chem Soc*. 2015;137:16008-16011.
140. Akkerman QA, Motti SG, Srimath Kandada AR, et al. Solution synthesis approach to colloidal cesium lead halide perovskite nanoplatelets with monolayer-level thickness control. *J Am Chem Soc*. 2016;138:1010-1016.
141. Lv L, Xu Y, Fang H, et al. Generalized colloidal synthesis of high-quality, two-dimensional cesium lead halide perovskite nanosheets and their applications in photodetectors. *Nanoscale*. 2016;8:13589-13596.
142. Song J, Xu L, Li J, et al. Monolayer and few-layer all-inorganic perovskites as a new family of two-dimensional semiconductors for printable optoelectronic devices. *Adv Mater*. 2016;28: 4861-4869.
143. Tong Y, Bladt E, Ayguler MF, et al. Highly luminescent cesium lead halide perovskite nanocrystals with tunable composition and thickness by ultrasonication. *Angew Chem Int Ed*. 2016;55:13887-13892.
144. Chen D, Chen X, Li J, Li X, Zhong J. Ultrathin $CsPbX_3$ (X = Cl, Br, I) nanoplatelets: solvothermal synthesis and optical spectroscopic properties. *Dalton Trans*. 2018;47:9845-9849.
145. Zhao J, Cao S, Li Z, Ma N. Amino acid-mediated synthesis of $CsPbBr_3$ perovskite nanoplatelets with Tunable thickness and optical properties. *Chem Mater*. 2018;30:6737-6743.
146. Kaniyankandy S, Vazhappilly T. Synthesis and electronic structure study on $CsPbBr_3$ nanoplatelets: thickness manipulation using surface ligands. *Colloids Surf A*. 2020;586: 124214.
147. Weidman MC, Goodman AJ, Tisdale WA. Colloidal halide perovskite nanoplatelets: an exciting new class of semiconductor nanomaterials. *Chem Mater*. 2017;29:5019-5030.
148. Vale BRC, Socie E, Burgos-Caminal A, Bettini J, Schiavon MA, Moser JE. Exciton, Biexciton, and hot exciton dynamics in $CsPbBr_3$ colloidal Nanoplatelets. *J Phys Chem Lett*. 2020;11:387-394.
149. Wang Q, Liu XD, Qiu YH, Chen K, Zhou L, Wang QQ. Quantum confinement effect and exciton binding energy of layered perovskite nanoplatelets. *AIP Adv*. 2018;8:025108.
150. Weidman MC, Seitz M, Stranks SD, Tisdale WA. Highly tunable colloidal perovskite nanoplatelets through variable cation, metal, and halide composition. *ACS Nano*. 2016;10: 7830-7839.
151. Li Q, Yang Y, Que W, Lian T. Size- and morphology-dependent auger recombination in $CsPbBr_3$ perovskite two-dimensional nanoplatelets and one-dimensional nanorods. *Nano Lett*. 2019;19:5620-5627.
152. Wang Y, Zhi M, Chang YQ, Zhang JP, Chan Y. Stable, ultralow threshold amplified spontaneous emission from $CsPbBr_3$ nanoparticles exhibiting trion gain. *Nano Lett*. 2018;18:4976-4984.
153. Wang S, Yu J, Zhang M, et al. Stable, strongly emitting cesium lead bromide perovskite nanorods with high optical gain enabled by an intermediate monomer reservoir synthetic strategy. *Nano Lett*. 2019;19:6315-6322.
154. Colvin VL, Schlamp MC, Alivisatos AP. Light-emitting-diodes made from cadmium selenide nanocrystals and a semiconducting polymer. *Nature*. 1994;370:354-357.
155. Tan ZN, Zhang F, Zhu T, et al. Bright and color-saturated emission from blue light-emitting diodes based on solution-processed colloidal nanocrystal quantum dots. *Nano Lett*. 2007;7:3803-3807.
156. Bae WK, Kwak J, Park JW, Char K, Lee C, Lee S. Highly efficient green-light-emitting diodes based on CdSe@ZnS quantum dots with a chemical-composition gradient. *Adv Mater*. 2009;21:1690-1694.
157. Zhang F, Wang S, Wang L, et al. Super color purity green quantum dot light-emitting diodes fabricated by using CdSe/CdS nanoplatelets. *Nanoscale*. 2016;8:12182-12188.
158. Giovanella U, Pasini M, Lorenzon M, et al. Efficient solution-processed nanoplatelet-based light-emitting diodes with high operational stability in air. *Nano Lett*. 2018;18:3441-3448.
159. Liu B, Sharma M, Yu J, et al. Light-emitting diodes with cu-doped colloidal quantum wells: from ultrapure green, tunable dual-emission to white light. *Small*. 2019;15:1901983.
160. Kim WD, Kim D, Yoon D-E, et al. Pushing the efficiency envelope for semiconductor nanocrystal-based electroluminescence devices using anisotropic nanocrystals. *Chem Mater*. 2019;31:3066-3082.
161. Wang Y, Fong KE, Yang SC, et al. Unraveling the ultralow threshold stimulated emission from CdZnS/ZnS quantum dot and enabling high-Q microlasers. *Laser Photon Rev*. 2015;9: 507-516.
162. Wang Y, Leck KS, Ta VD, et al. Blue liquid lasers from solution of CdZnS/ZnS ternary alloy quantum dots with quasi-continuous pumping. *Adv Mater*. 2015;27:169-175.
163. Zavelani-Rossi M, Lupo MG, Krahne R, Manna L, Lanzani G. Lasing in self-assembled microcavities of CdSe/CdS core/shell colloidal quantum rods. *Nanoscale*. 2010;2:931-935.
164. Naskar S, Schlosser A, Miethe JF, Steinbach F, Feldhoff A, Bigall NC. Site-selective noble metal growth on CdSe nanoplatelets. *Chem Mater*. 2015;27:3159-3166.
165. Chauhan H, Kumar Y, Dana J, Satpati B, Ghosh HN, Deka S. Photoinduced ultrafast charge separation in colloidal 2-dimensional CdSe/CdS-Au hybrid nanoplatelets and corresponding application in photocatalysis. *Nanoscale*. 2016; 8:15802-15812.
166. Gao F, Yang L, Tang J, et al. Fin-like CdSeS nanoplatelets for pesticide sensing. *ACS Appl Nano Mater*. 2019;2:3459-3466.

AUTHOR BIOGRAPHIES

Jiahao Yu received his MS degree in Materials Science and Engineering from Wuhan University of Technology in 2017. He is currently pursuing the Joint PhD degree between Harbin Institute of Technology and Southern University of Science and Technology, under the supervision of Prof. Rui Chen. His current research interests include the optical properties of semiconductor nanomaterials and their applications.

Rui Chen received PhD degree in applied physics from Nanyang Technological University, and physics from Xiamen University, respectively. He is currently working at Department of Electrical and Electronic Engineering at Southern University of Science and Technology. His research interests include the laser spectroscopy, optical properties of materials, optical microcavity, and micro/nano lasers.

How to cite this article: Yu J, Chen R. Optical properties and applications of two-dimensional CdSe nanoplatelets. *InfoMat*. 2020;2:905–927. https://doi.org/10.1002/inf2.12106